

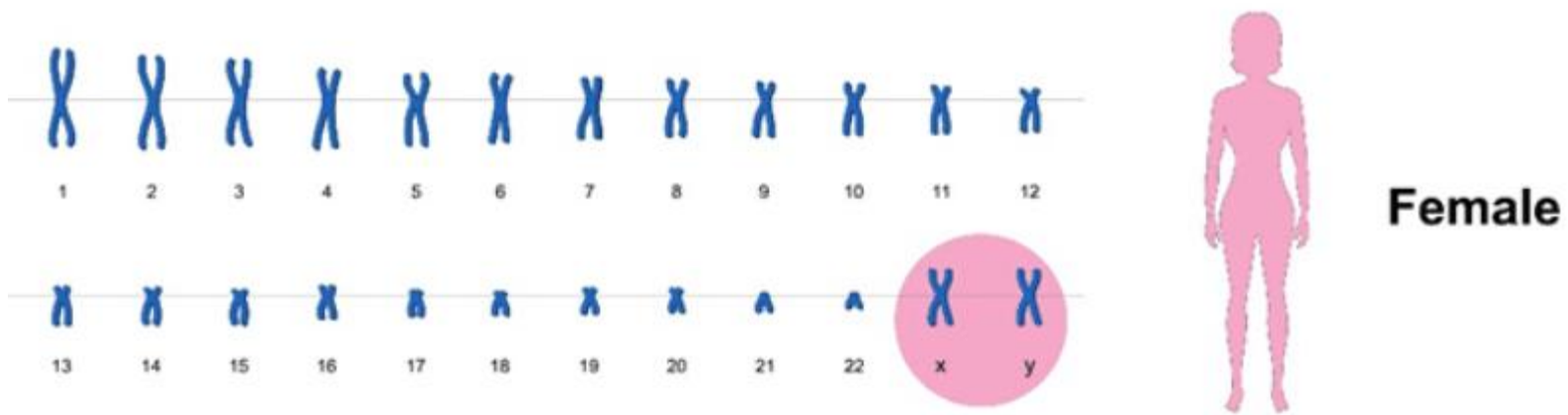
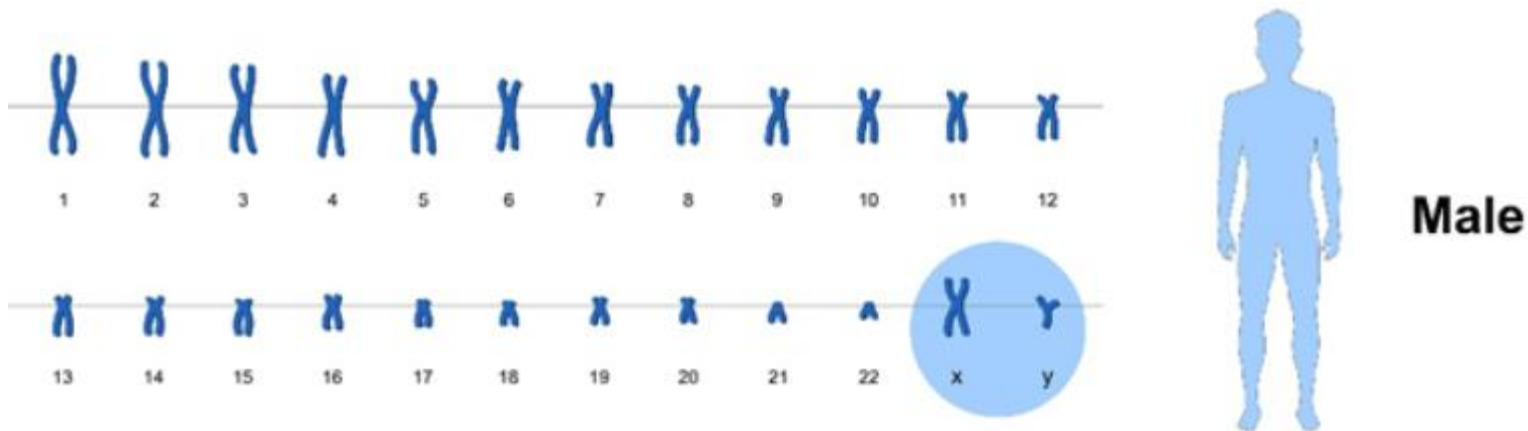
## Medical/Bio Research Topics II: Week 12 (21.11.2025)

# **Hands-on AI Classification Model Development (1): Data and Prediction Problem**

**인공지능 분류 모델 개발 실습 (1): 데이터 및 예측 문제**

# Sex and Gender

- Sex
  - Usually described by the terms "males" and "females"
  - Typically refers to the biological and physiological characteristics that define males and females
  - Determined by biological factors, primarily chromosomal (XX for females, XY for males) and anatomical differences



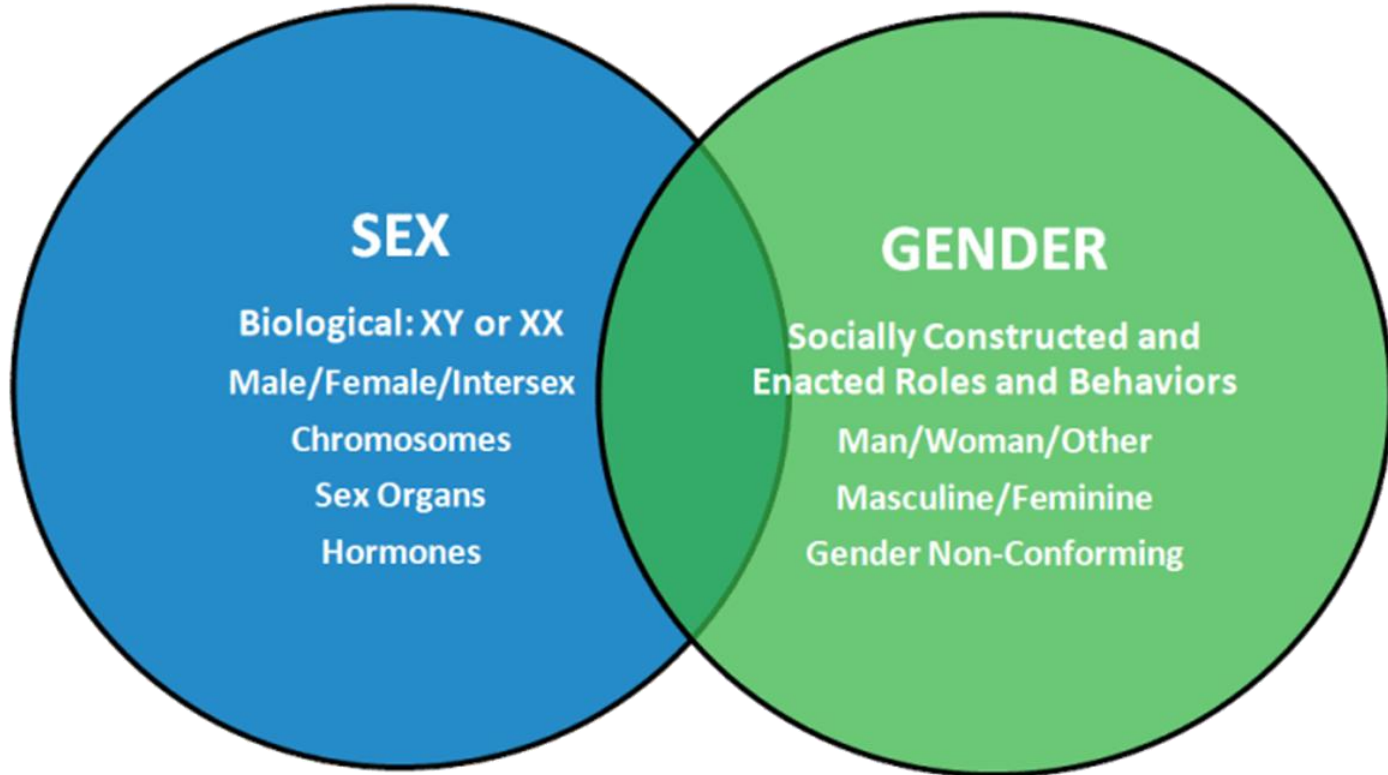
[<https://www.shalom-education.com/courses/gcse-biology/lessons/genetic-variation-and-mutation/topic/sex-determination>]

## Sex Determination Through Sex Chromosomes



Intersex Born with Sex Characteristics that Do Not Fit Typical Binary Notions

- Gender
  - Usually described by the terms "men" and "women"
  - Often refers to the socially constructed roles, behaviors, activities, and attributes that a society considers appropriate for individuals based on their sex
  - Related to how individuals perceive themselves and what they call themselves, which can be influenced by societal norms and personal experiences
- Both sex and gender exist on a spectrum, such that individuals may identify and express themselves in various ways that do not conform to traditional binary categories

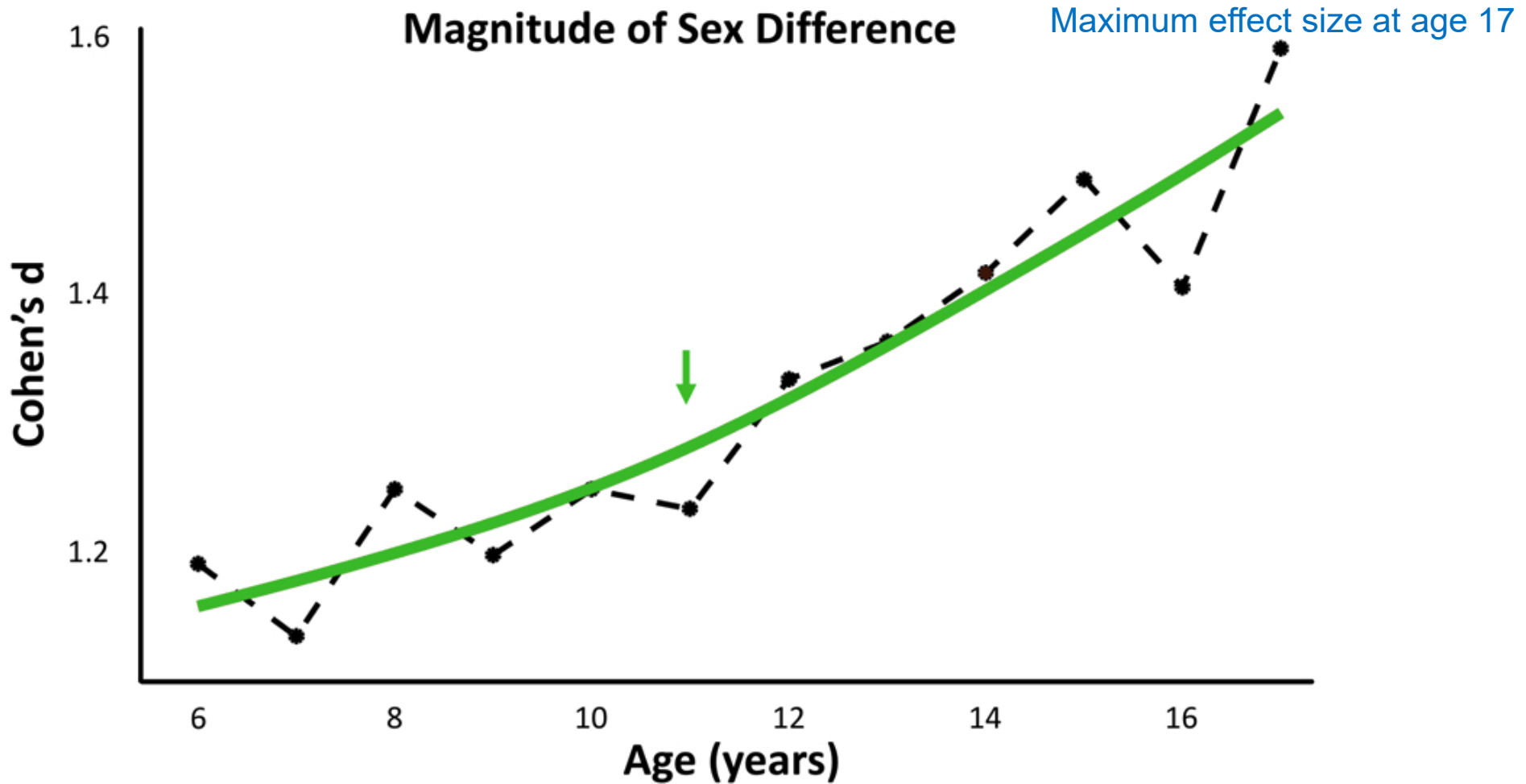


[<https://orwh.od.nih.gov/sex-gender>]

## Dimensions of Sex and Gender

# Sex Differences in Brain Structure

- Described from early childhood through late adulthood
  - Systematic sex difference in brain structure already during childhood, and a subsequent increase of this difference during adolescence [\[Kurth et al., 2020\]](#)
- Brain sex
  - Brain-specific number on a scale of 0 (100% female brain) to 1 (100% male brain)
    - Continuous probabilistic estimate of the degree of maleness or femaleness

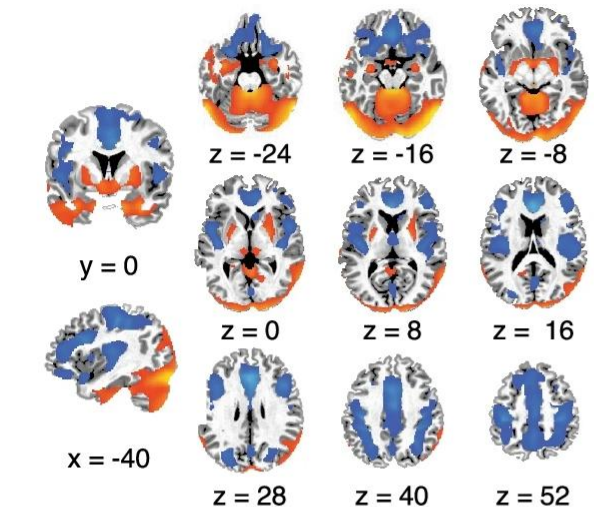


[Sanchis-Segura et al., 2019]

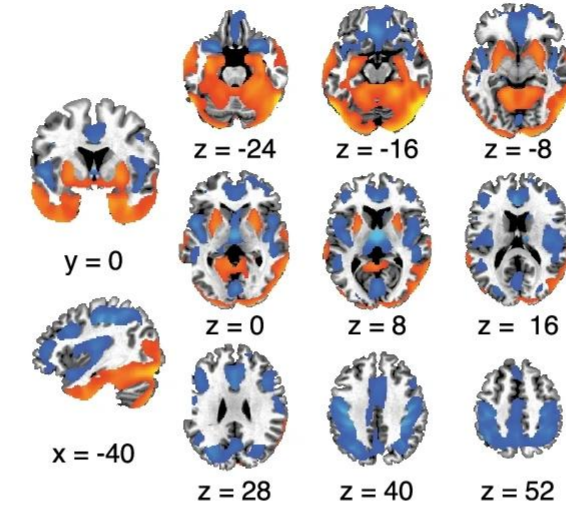
**Age-specific Sex Differences**

- Lack of clear consensus among studies
  - Within-sex individual variability and the limited applicability of group findings to individuals
  - Biological and environmental factor interactions in shaping sex differences across brain regions
  - Probable absence of direct correspondence between sex-based brain region differences and clear-cut behavioral manifestations

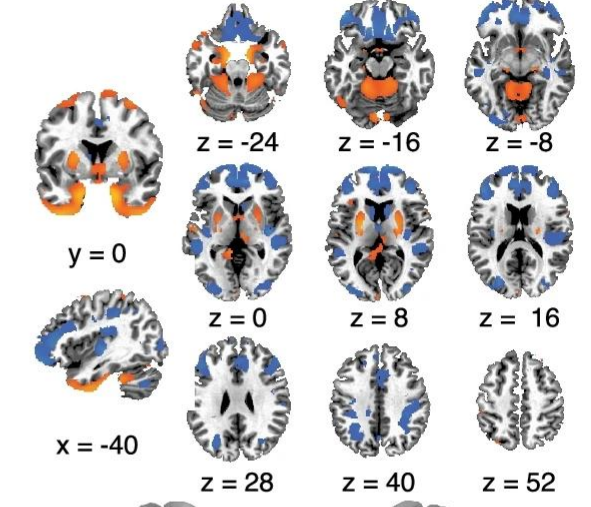
**Significant sex differences in HCP  
(United States; N = 976)**



**Significant sex differences in UKB  
(United Kingdom; N = 1,120)**



**Significant sex differences in Lotze  
(Germany; N = 2,838)**



[DeCasien et al., 2022]

**Sex Differences in Brain Structure Across Three Large Cohorts: Males vs. Females**

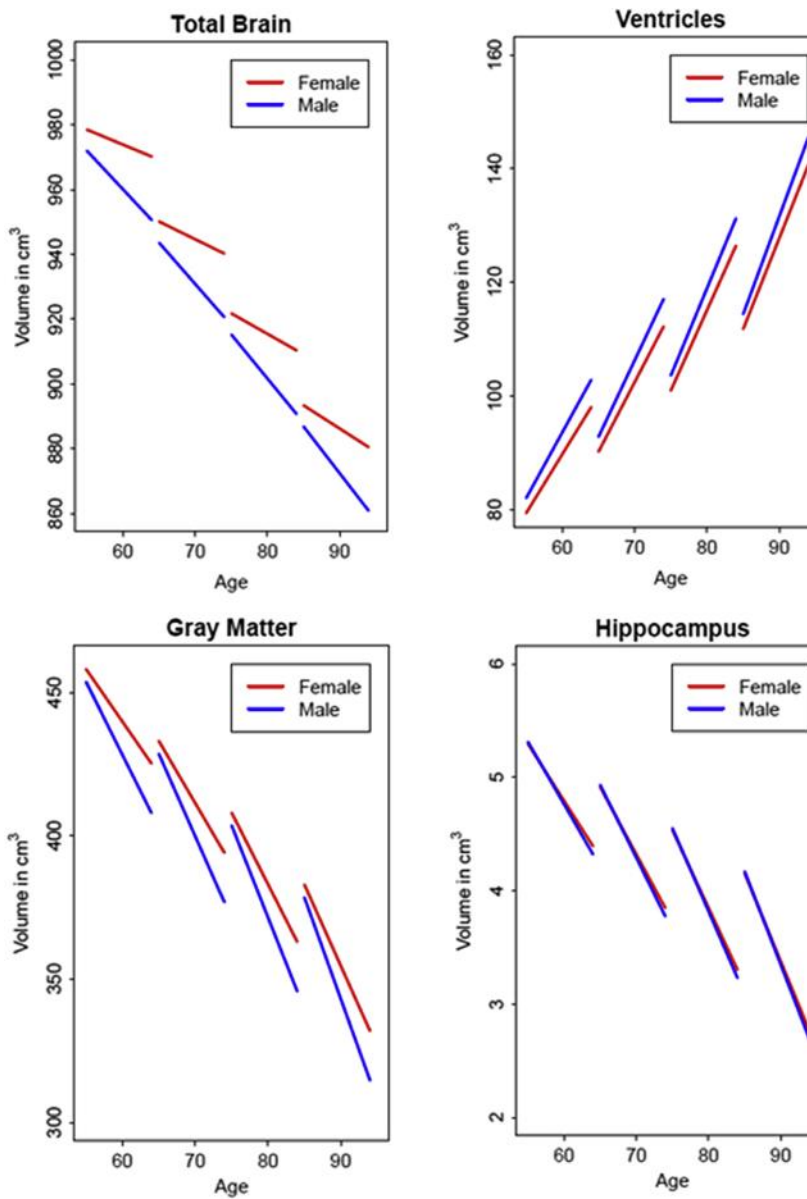
# Sex Differences in Brain Aging

- Sex differences in age-related brain changes
  - Greater regional brain volume changes in males than females [Coffey et al., 1998]
  - Steeper regional brain volume changes with older age in both sexes, with men showing consistently greater changes than women across the later life span [Armstrong et al., 2019]
  - Earlier onset of age-related white matter microstructural degeneration in males than females [Toschi et al., 2020]

	Age, y						
	65	70	75	80	85	90	95
Peripheral CSF volume, mL							
Men	199.36	209.90	220.43	230.97	241.50	252.03	262.57
Women	205.06	205.37	205.68	205.98	206.29	206.59	206.90
Lateral fissure CSF volume, mL							
Men	8.70	9.86	11.02	12.19	13.35	14.51	15.68
Women	7.90	8.38	8.87	9.36	9.85	10.34	10.82
Parieto-occipital region area, cm <sup>2</sup>							
Men	62.79	61.23	59.66	58.10	56.54	54.97	53.40
Women	60.64	60.18	59.74	59.29	58.84	58.39	57.94

[Coffey et al., 1998]

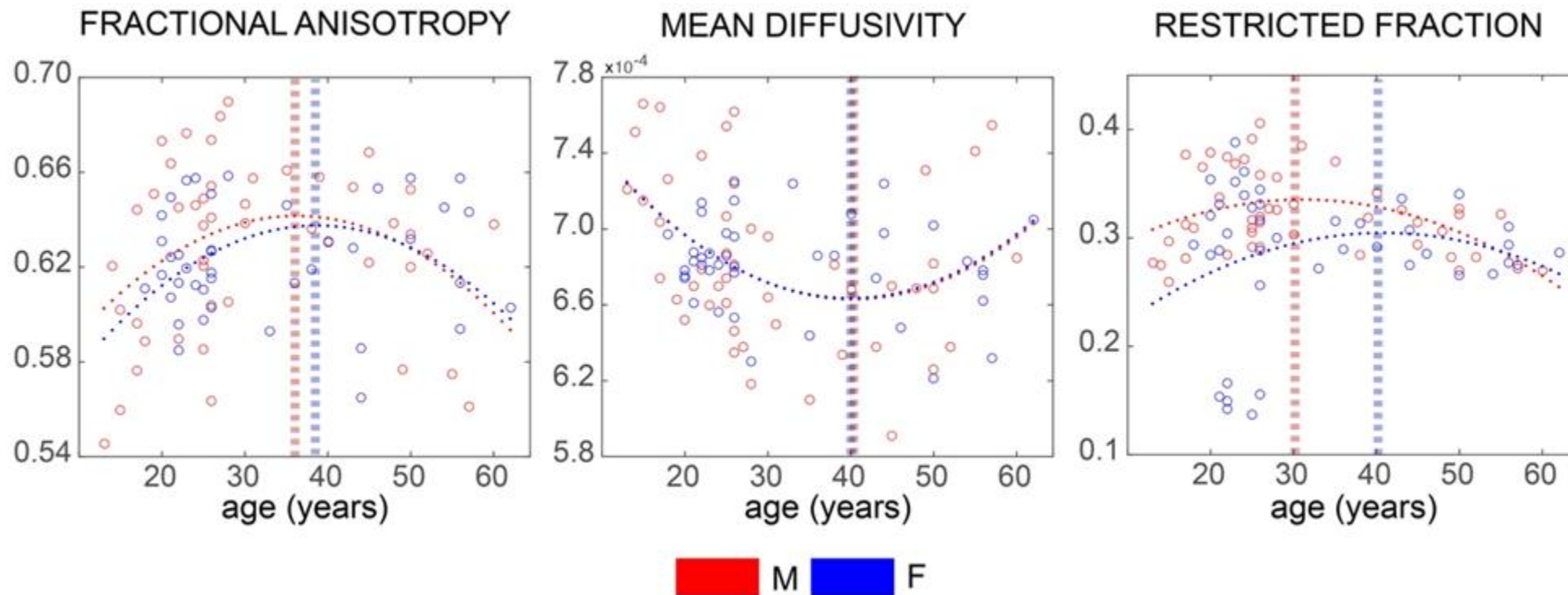
## Sex Differences in Age-related Regional Brain Volume Changes



[Armstrong et al., 2019]

## Sex-specific Trajectories of Regional Brain Volume Changes by Five-year Age Intervals

■ Age at which diffusion metrics invert their development trend



[Toschi et al., 2020]

**Sex-specific Trajectories of White Matter Microstructure Changes**

# Classification in Machine Learning

- Models the relationship between input features (predictors) and one or more target variables
- Purpose
  - Understanding the relationship between input features and categorical target variables
  - Predicting categorical target values (class labels) for new sets of input features

- Supervised learning technique for predicting discrete output values (class labels)
  - Traditional methods
    - Linear classification: Logistic regression, linear discriminant analysis (LDA)
    - Non-linear classification: Support vector machines (SVM) with non-linear kernels, k-nearest neighbors (k-NN), decision trees, naive Bayes
  - Ensemble methods
    - Bagging-based methods: random forests, Extra Trees (extremely randomized trees)
    - Boosting-based methods: AdaBoost (adaptive boosting), gradient boosting machines (GBM), XGBoost (extreme gradient boosting), LightGBM (light gradient boosting machine), CatBoost (categorical boosting)
    - Stacking: combining predictions from multiple models

- Deep learning methods
  - Feedforward neural network (FNN) / multilayer perceptron (MLP)
  - Specialized architectures
    - Convolutional neural network (CNN) for spatial data classification
    - Recurrent neural network (RNN) and long short-term memory (LSTM) for sequential data classification
  - Transformer-based models for complex sequential data classification
- Hybrid approaches
  - Combining traditional methods with ensemble techniques or neural networks
  - Automated machine learning (AutoML) systems incorporating various classification techniques

- Types of classification problems
  - Based on the nature of the relationship
    - Linear classification: modeling linear decision boundaries
    - Nonlinear classification: modeling complex, nonlinear decision boundaries
  - Based on the number of output variables
    - Single-output classification: predicting one categorical variable
      - Binary: two classes (e.g., spam vs. not spam)
      - Multi-class: more than two classes (e.g., animal species)
    - Multi-output classification: predicting multiple categorical variables simultaneously
      - Multi-label: multiple binary variables (e.g., image tagging)
      - Multi-class multi-output: multiple multi-class variables (e.g., predicting both weather and time of day)

- Classification performance

- Accuracy

- Proportion of correct predictions among the total number of cases examined:  $(TP + TN) / (TP + FP + TN + FN)$
    - Range: 0 to 1 (higher is better)
    - Easy to interpret, but can be misleading for imbalanced datasets

- Precision (true positive value (TPV))

- Proportion of true positive predictions among all positive predictions:  $TP / (TP + FP)$
    - Range: 0 to 1 (higher is better)
    - Focuses on the accuracy of positive predictions

- Recall (true positive rate (TPR) or sensitivity)
  - Proportion of true positive predictions among all actual positive cases:  $TP / (TP + FN)$
  - Range: 0 to 1 (higher is better)
  - Focuses on the completeness of positive predictions
- $F_1$  score
  - Harmonic mean of precision and recall:  $2 / ((1 / \text{precision}) + (1 / \text{recall})) = 2TP / (2TP + FP + FN)$
  - Range: 0 to 1 (higher is better)
  - Provides a single score that balances both precision and recall
  - Particularly useful for imbalanced datasets

		Predicted condition	
		Positive (PP)	Negative (PN)
Total population $= P + N$		Positive (PP)	Negative (PN)
Actual condition	Positive (P)	True positive (TP), hit	False negative (FN), type II error, miss, underestimation
	Negative (N)	False positive (FP), type I error, false alarm, overestimation	True negative (TN), correct rejection

[[https://en.wikipedia.org/wiki/Confusion\\_matrix](https://en.wikipedia.org/wiki/Confusion_matrix)]

## Confusion Matrix: Special Kind of Contingency Table

- Receiver operating characteristic (ROC) curve
  - Graph showing the performance of a classification model at all classification thresholds
  - Plots TPR (TPR, sensitivity) against false positive rate ( $FPR = 1 - \text{true negative rate (TNR, specificity)}$ )
  - Useful for visualizing the trade-off between sensitivity and specificity
- Area under the ROC curve (AUC-ROC)
  - Aggregate measure of performance across all possible classification thresholds
  - Range: 0.5 (random guessing) to 1 (perfect classification)
  - Provides a single score that summarizes the ROC curve

## – Confusion matrix

- Table showing the number of true positives, true negatives, false positives, and false negatives
- Not a single metric, but a comprehensive view of the model's performance
- Useful for deriving other metrics and understanding the types of errors made

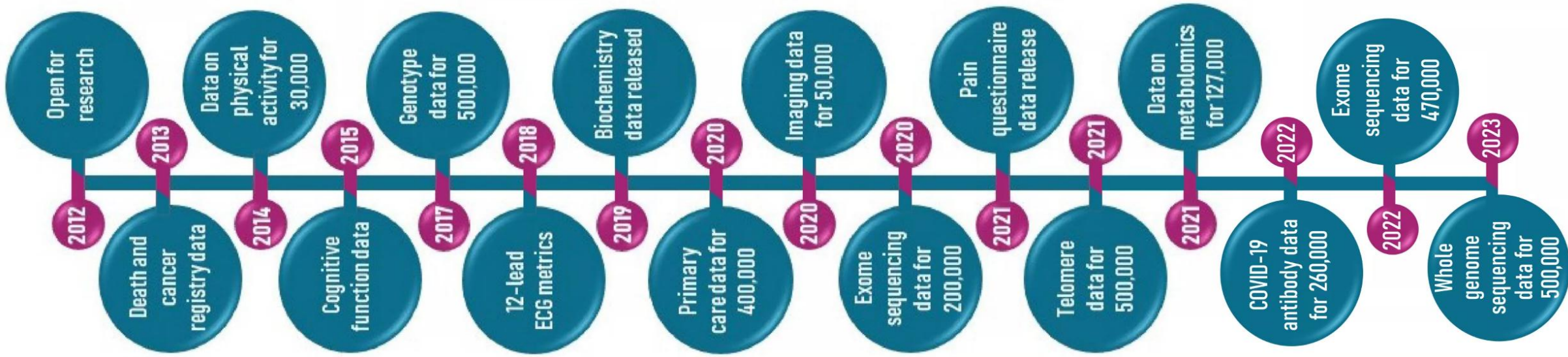
		Predicted condition			
		Positive (PP)	Negative (PN)	Informedness, bookmaker informedness (BM) = TPR + TNR - 1	Prevalence threshold (PT) $= \frac{\sqrt{TPR \times FPR} - FPR}{TPR - FPR}$
Actual condition	Positive (P)	True positive (TP), hit	False negative (FN), type II error, miss, underestimation	True positive rate (TPR), recall, sensitivity (SEN), probability of detection, hit rate, power $= \frac{TP}{P} = 1 - FNR$	False negative rate (FNR), miss rate $= \frac{FN}{P} = 1 - TPR$
	Negative (N)	False positive (FP), type I error, false alarm, overestimation	True negative (TN), correct rejection	False positive rate (FPR), probability of false alarm, fall-out $= \frac{FP}{N} = 1 - TNR$	True negative rate (TNR), specificity (SPC), selectivity $= \frac{TN}{N} = 1 - FPR$
Prevalence $= \frac{P}{P + N}$	Positive predictive value (PPV), precision $= \frac{TP}{PP} = 1 - FDR$	False omission rate (FOR) $= \frac{FN}{PN} = 1 - NPV$	Positive likelihood ratio (LR+) $= \frac{TPR}{FPR}$	Negative likelihood ratio (LR-) $= \frac{FNR}{TNR}$	
Accuracy (ACC) $= \frac{TP + TN}{P + N}$	False discovery rate (FDR) $= \frac{FP}{PP} = 1 - PPV$	Negative predictive value (NPV) $= \frac{TN}{PN} = 1 - FOR$	Markedness (MK), deltaP ( $\Delta p$ ) $= PPV + NPV - 1$	Diagnostic odds ratio (DOR) $= \frac{LR+}{LR-}$	
Balanced accuracy (BA) $= \frac{TPR + TNR}{2}$	F <sub>1</sub> score $= \frac{2PPV \times TPR}{PPV + TPR} = \frac{2TP}{2TP + FP + FN}$	Fowlkes–Mallows index (FM) $= \sqrt{PPV \times TPR}$	Matthews correlation coefficient (MCC) $= \sqrt{TPR \times TNR \times PPV \times NPV} - \sqrt{FNR \times FPR \times FOR \times DFR}$	Threat score (TS), critical success index (CSI), Jaccard index $= \frac{TP}{TP + FN + FP}$	

[[https://en.wikipedia.org/wiki/Confusion\\_matrix](https://en.wikipedia.org/wiki/Confusion_matrix)]

## Confusion Matrix and Its Derived Metrics

# UK Biobank

- World's largest health research database
  - Around 500,000 UK residents aged 40-69 years at recruitment
  - Initial recruitment from 2006 to 2010
  - Ongoing follow-up:
    - Regular updates of health outcomes for all participants
    - Ongoing imaging study, aiming to scan 100,000 participants
    - Periodic questionnaires on various health topics
- Aims to improve prevention, diagnosis, and treatment of various diseases



[<https://www.ukbiobank.ac.uk/enable-your-research/about-our-data>]

## Extension of UK Biobank Data

- Unique features
  - Large sample size
  - Comprehensive data collection
  - Long-term follow-up
- Types of data collected
  - Genetic information: whole genome sequencing, whole exome sequencing, and genotyping
  - Health-related records
  - Lifestyle questionnaires
  - Physical measurements
  - Imaging data (for a subset of participants)

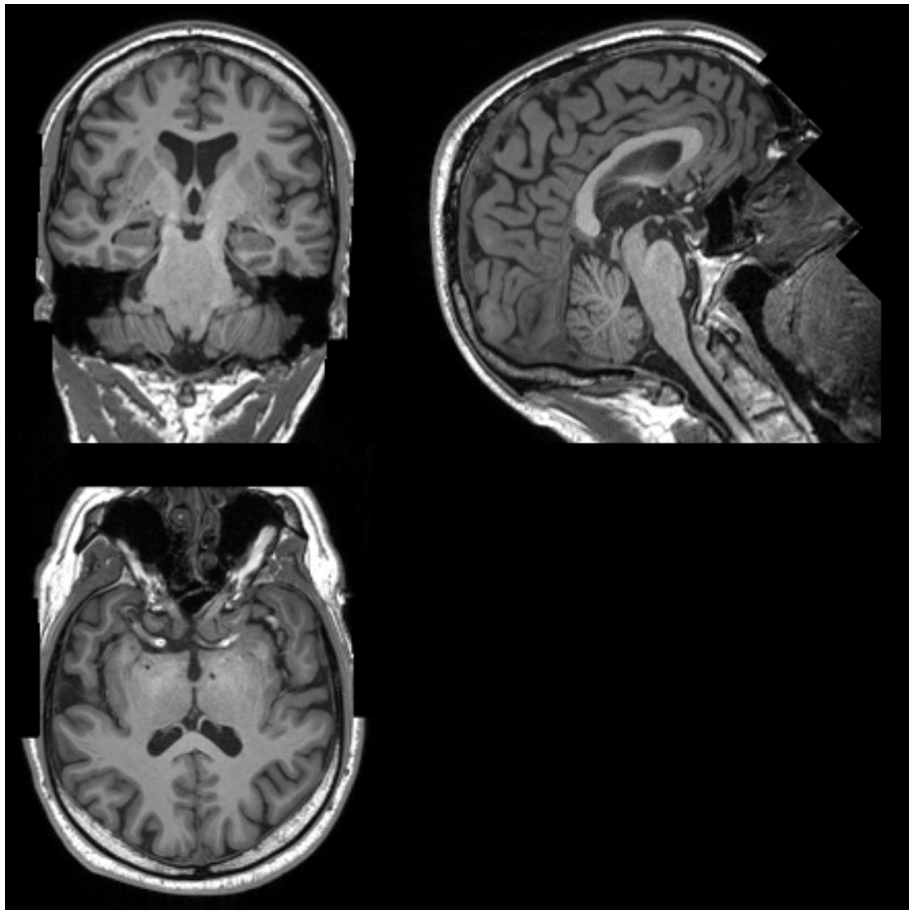
- Brain MRI data
  - Structural MRI (sMRI)
    - T1-weighted
    - FLAIR
  - Functional MRI (fMRI)
    - Task-based
    - Resting-state
  - Diffusion-weighted MRI (dMRI)
  - Susceptibility-weighted MRI (swMRI)

Modality	Duration	Voxel, Matrix	Key Parameters	#Volumes/ #Timepoints
T1	4:54	$1 \times 1 \times 1$ mm $208 \times 256 \times 256$	3D MPRAGE, sagittal, R = 2, TI/TR = 880/ 2000 ms	1
T2	5:52	$1.05 \times 1.0 \times 1.0$ mm $192 \times 256 \times 256$	FLAIR, 3D SPACE, sagittal, R = 2, PF 7/ 8, fat sat, TI/ TR = 1800/5000 ms, elliptical	1
swMRI	2:34	$0.8 \times 0.8 \times 3.0$ mm $256 \times 288 \times 48$	3D GRE, axial, R = 2, PF 7/8 TE1/TE2/ TR = 9.4/20/27 ms	2
dMRI	7:08	$2.0 \times 2.0 \times 2.0$ mm $104 \times 104 \times 72$	MB = 3, R = 1, TE/ TR = 92/3600 ms, PF 6/8, fat sat, b = 0 $s/mm^2$ (5x + 3x phase-encoding reversed), b = 1 000 $s/mm^2$ (50×), b = 2000 $s/mm^2$ (50×)	105 + 6 (AP + PA)
rfMRI	6:10	$2.4 \times 2.4 \times 2.4$ mm $88 \times 88 \times 64$	TE/TR = 39/735 ms, MB = 8, R = 1, flip angle 52°, fat sat	490
tfMRI	4:13	$2.4 \times 2.4 \times 2.4$ mm $88 \times 88 \times 64$	Acquisition same as rfMRI. Task is faces/ shapes “emotion” task.	332

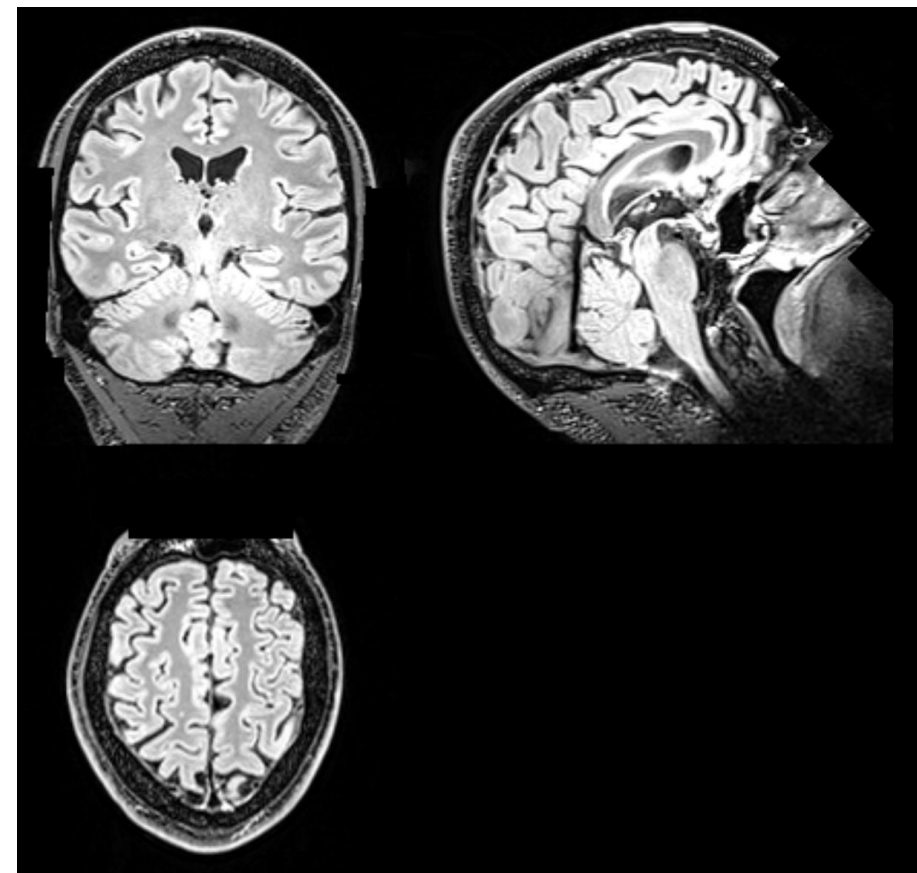
[Alfaro-Almagro et al., 2018]

## Brain MRI Data in UK Biobank

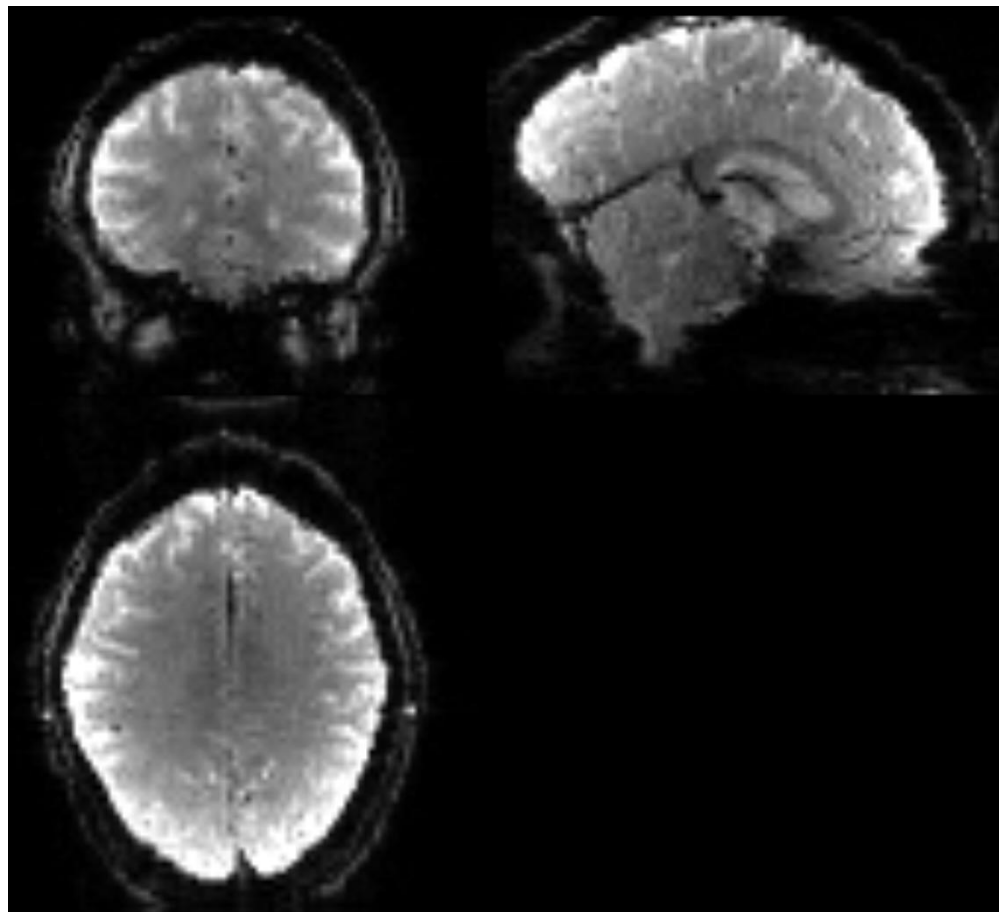
T1-weighted sMRI



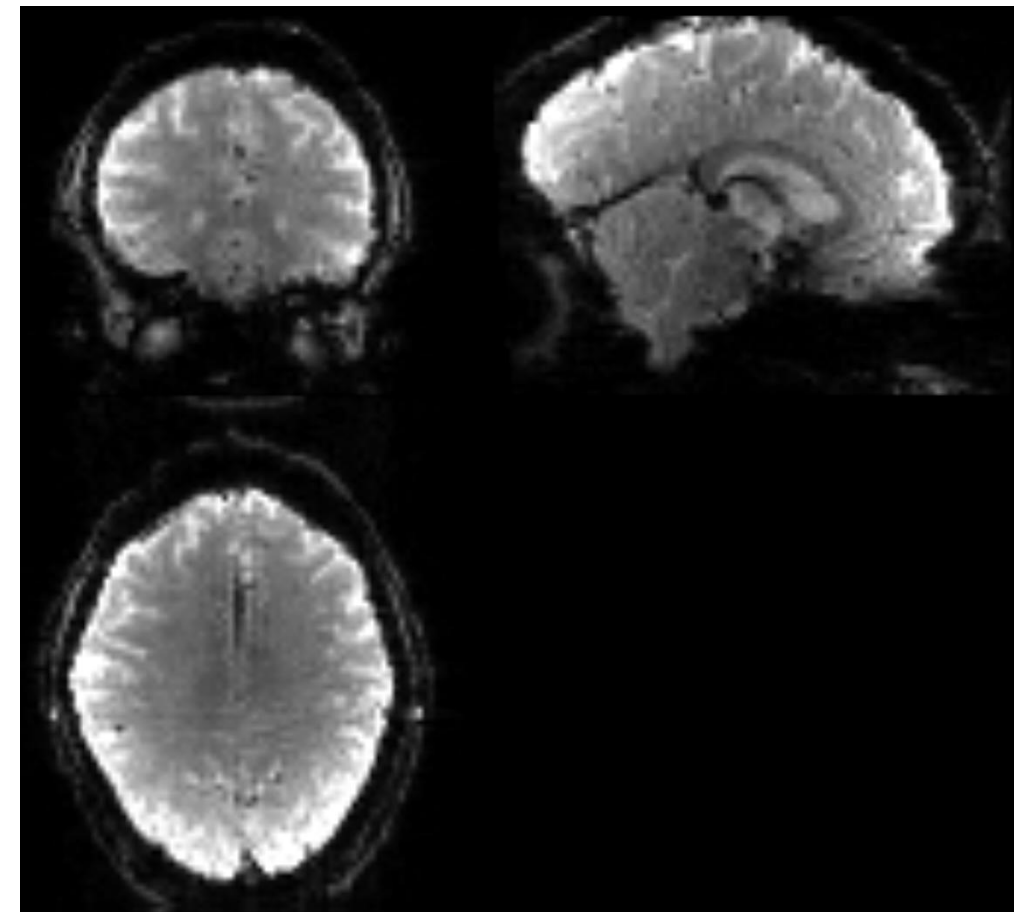
FLAIR sMRI



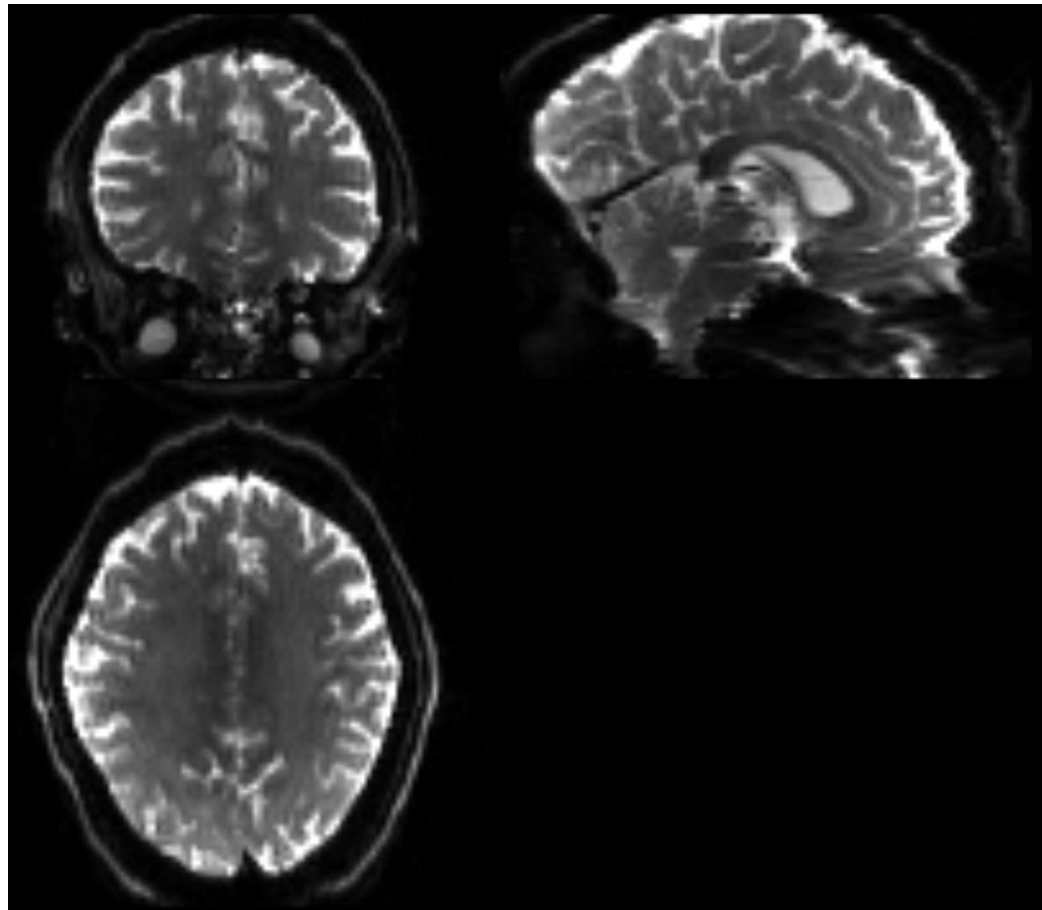
Task-based fMRI



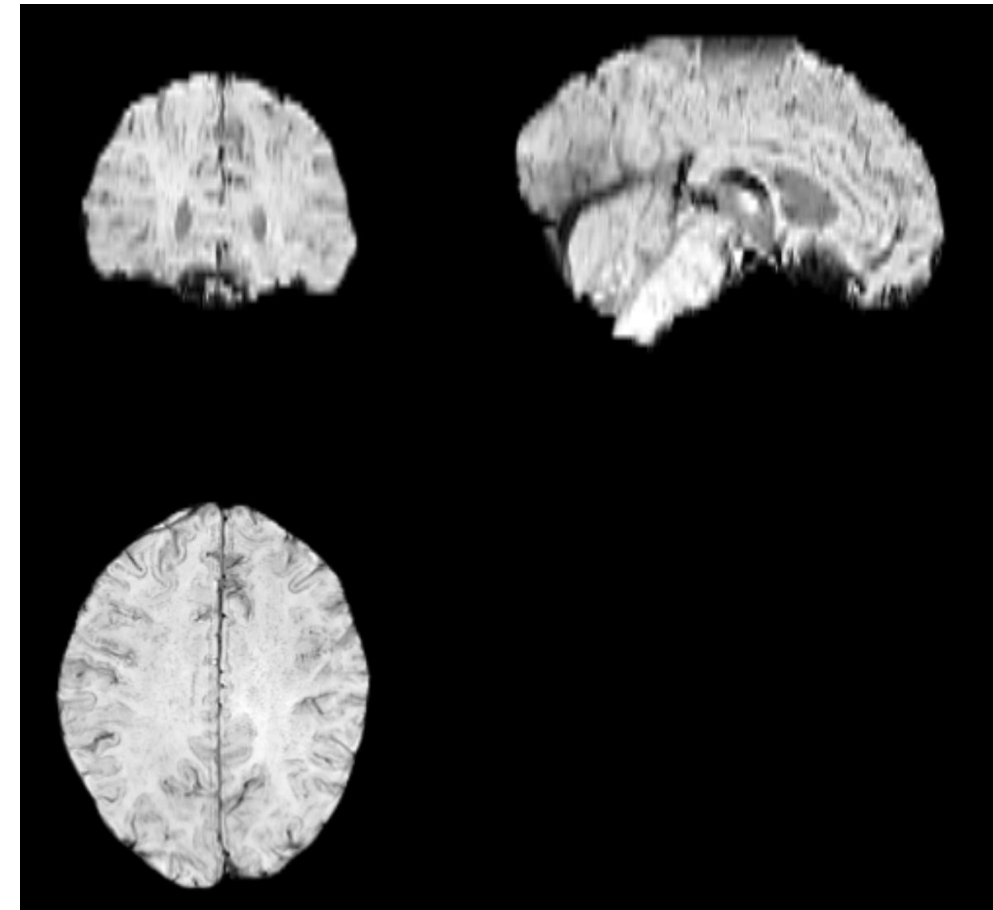
Resting-state fMRI



dMRI



swMRI

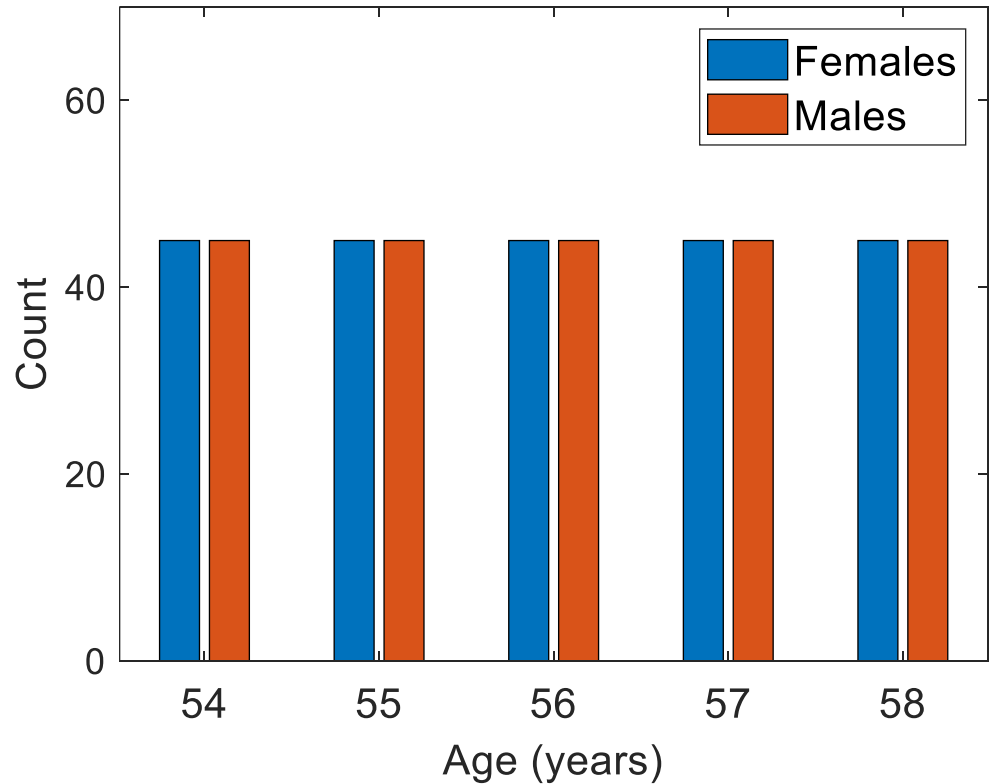


# Dataset

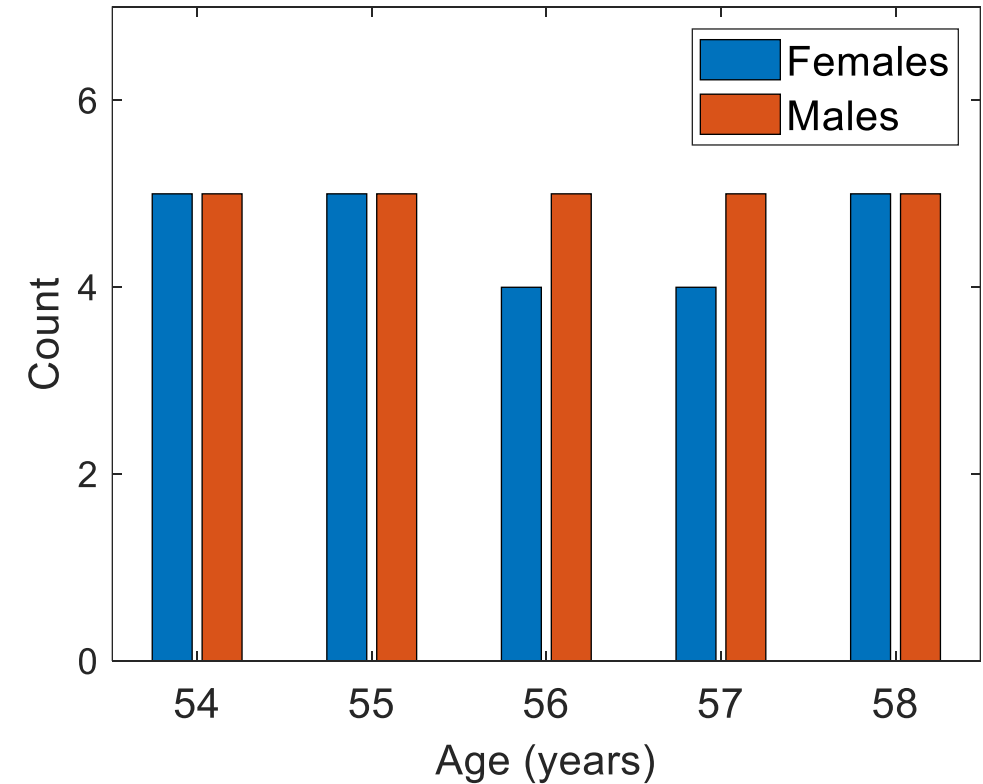
- Part of UK Biobank dataset ( $n = 498$ )
  - Training set:  $n = 450$ 
    - Functional brain networks from resting-state fMRI data: [train/{PC,GC}/001-450.csv](#)
    - Network metrics for functional brain networks:  
[train/{FuncBU\\_GE,FuncBU\\_LE,FuncBD\\_GE,FuncBD\\_LE}/001-450.csv](#)
    - Structural brain networks from dMRI data:  
[train/{Count,FA,MD,AD,RD}/001-450.csv](#)
    - Network metrics for structural brain networks:  
[train/{StruBU\\_GE,StruBU\\_LE}/001-450.csv](#)

- Age (in years): [train/Subjects.csv](#): Age
  - Sex (0: female, 1: male): [train/Subjects.csv](#): Sex
- Test set:  $n = 48$
- Functional brain networks from resting-state fMRI data: [test/{PC,GC}/001-048.csv](#)
  - Network metrics for functional brain networks:  
[test/{FuncBU\\_GE,FuncBU\\_LE,FuncBD\\_GE,FuncBD\\_LE}/001-048.csv](#)
  - Structural brain networks from dMRI data: [test/{Count,FA,MD,AD,RD}/001-048.csv](#)
  - Network metrics for structural brain networks:  
[test/{StruBU\\_GE,StruBU\\_LE}/001-048.csv](#)
  - Age (in years): [test/Subjects.csv](#): Age
  - Sex (0: female, 1: male): hidden

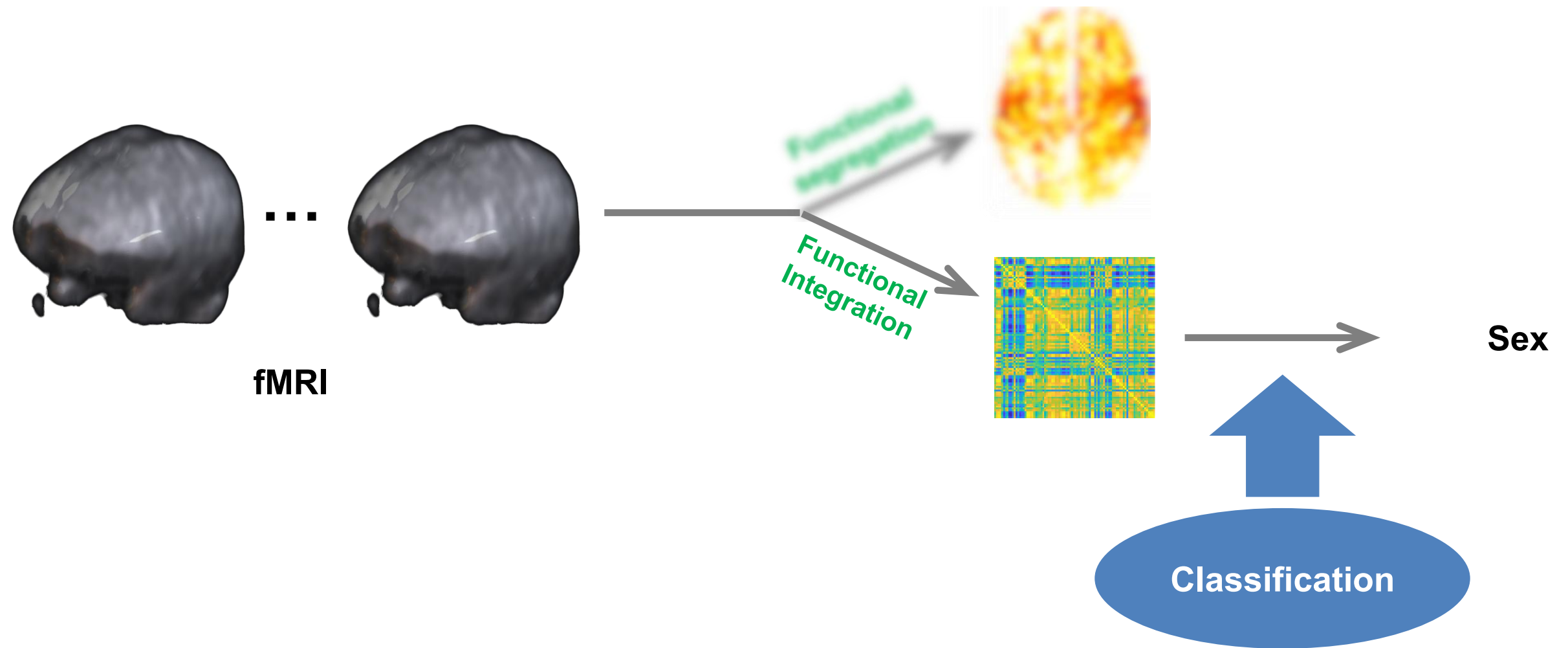
Training set



Test set

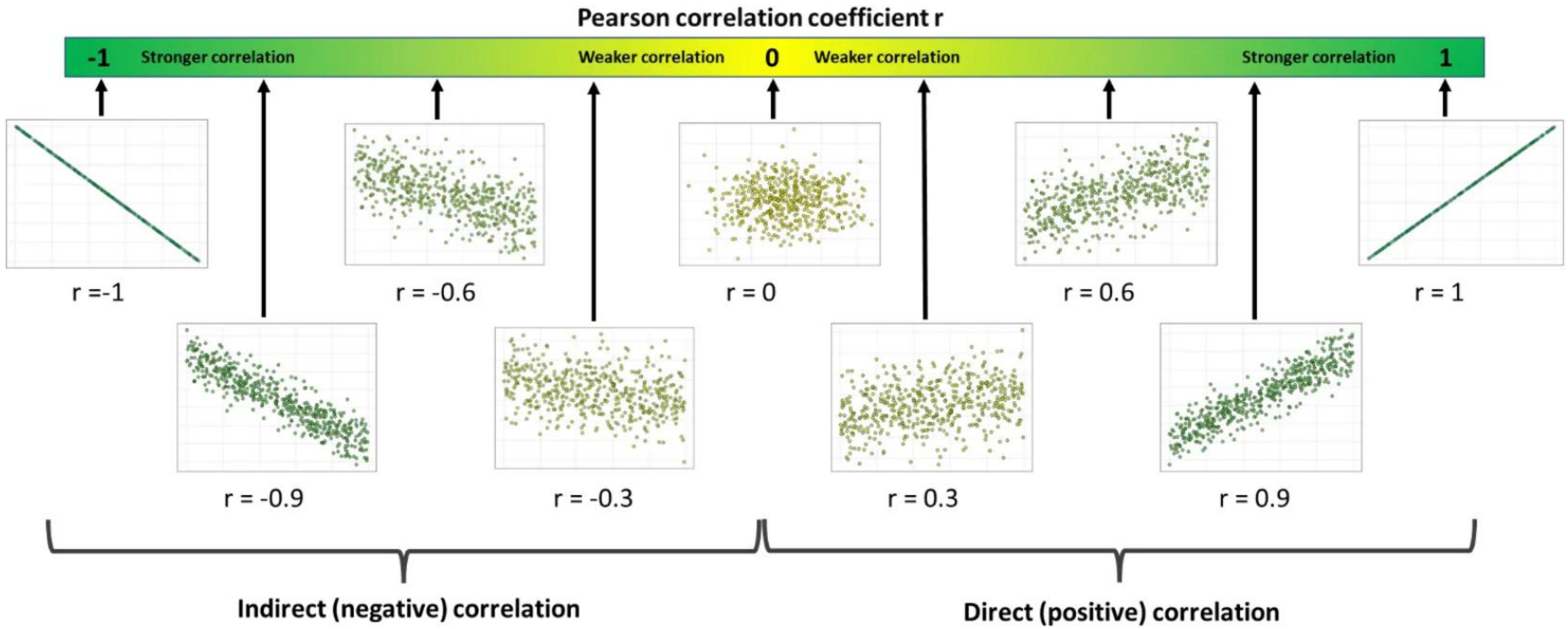


**Distribution of Age and Sex for Training and Test Sets**



- Preprocessing of resting-state fMRI data
  - Correction for slice timing difference, head motion, and susceptibility artifact (B0 inhomogeneity-induced distortion)
  - Extraction of time series
  - Construction of functional brain networks
    - Nodes: pre-defined brain regions
    - Edges: connectivity (correlation or causality) between brain regions

- Pearson correlation
  - Measures the linear relationship (strength and direction) between two variables
  - Characteristics:
    - Range: -1 to 1
    - Symmetric
    - Does not imply causation
  - Computed by effectively standardizing the covariance between two variables (how the two variables change together) by dividing it by the product of the two standard deviations
  - Useful for identifying potential associations between variables, but not accounting for time lags or temporal order



[<https://medium.com/@anthony.demeusy/pearson-correlation-methodology-limitations-alternatives-part-1-methodology-42abe8f1ba90>]

## Range of Pearson Correlation Coefficient

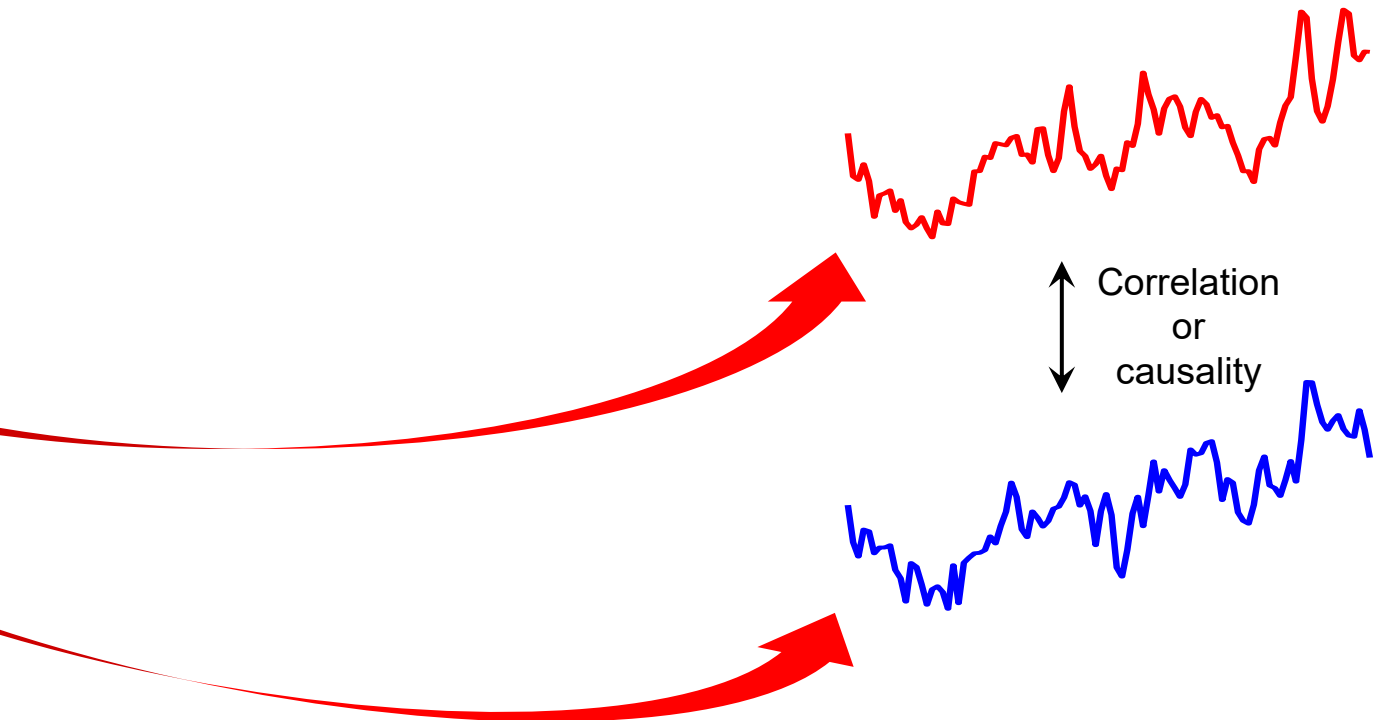
- Granger causality
  - Tests predictive causality (whether one time series is useful in forecasting another time series)
  - Characteristics:
    - Asymmetric
    - Considers temporal order and lags
  - Useful for understanding temporal relationships in time series, but not necessarily implying true causation

- Computed by comparing models with and without the potential causal variable based on autoregressive models that predict a variable's current value based on its own past values
  - Choose a maximum lag length
  - For each lag length up to the maximum:
    - Create two regression models: restricted model that predicts Y using only past values of Y (autoregressive) vs. unrestricted model that predicts Y using past values of both Y and X (augmented autoregressive)
    - Estimate both models and compute the  $F$ -statistic and its associated  $p$ -value
  - Compare the  $p$ -values to the chosen significance level
    - If the  $p$ -value is below the significance level (typically 0.05), conclude that X Granger-causes Y for that lag length
  - Repeat the process across different lag lengths



[Fan et al., 2016]

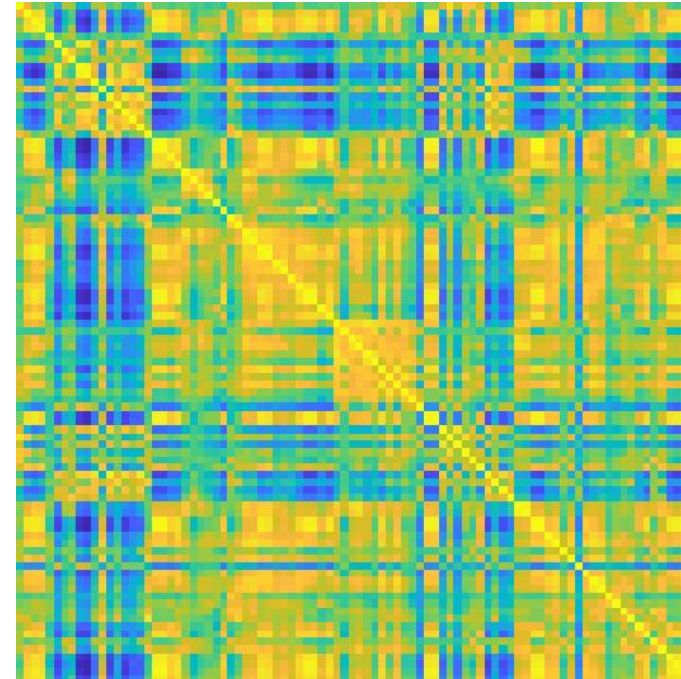
**Definition of 246 Nodes Based on the Brainnetome Atlas**



**Estimation of Edges Between 246 Nodes**

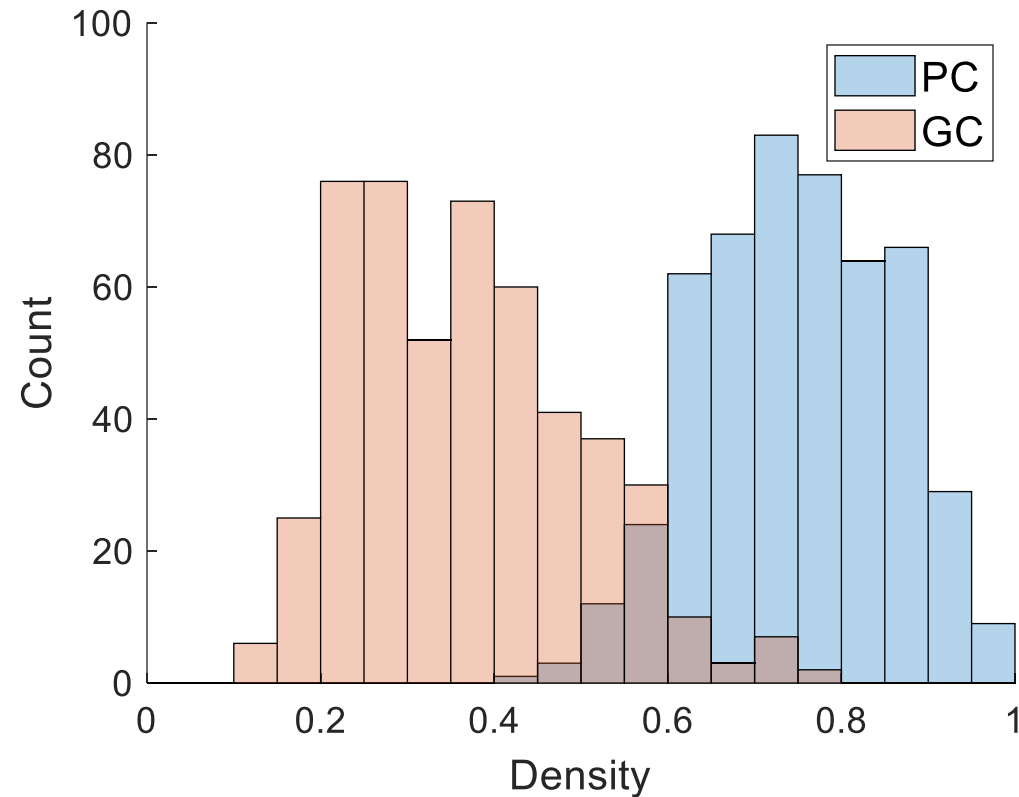


Time series  
correlation or causality

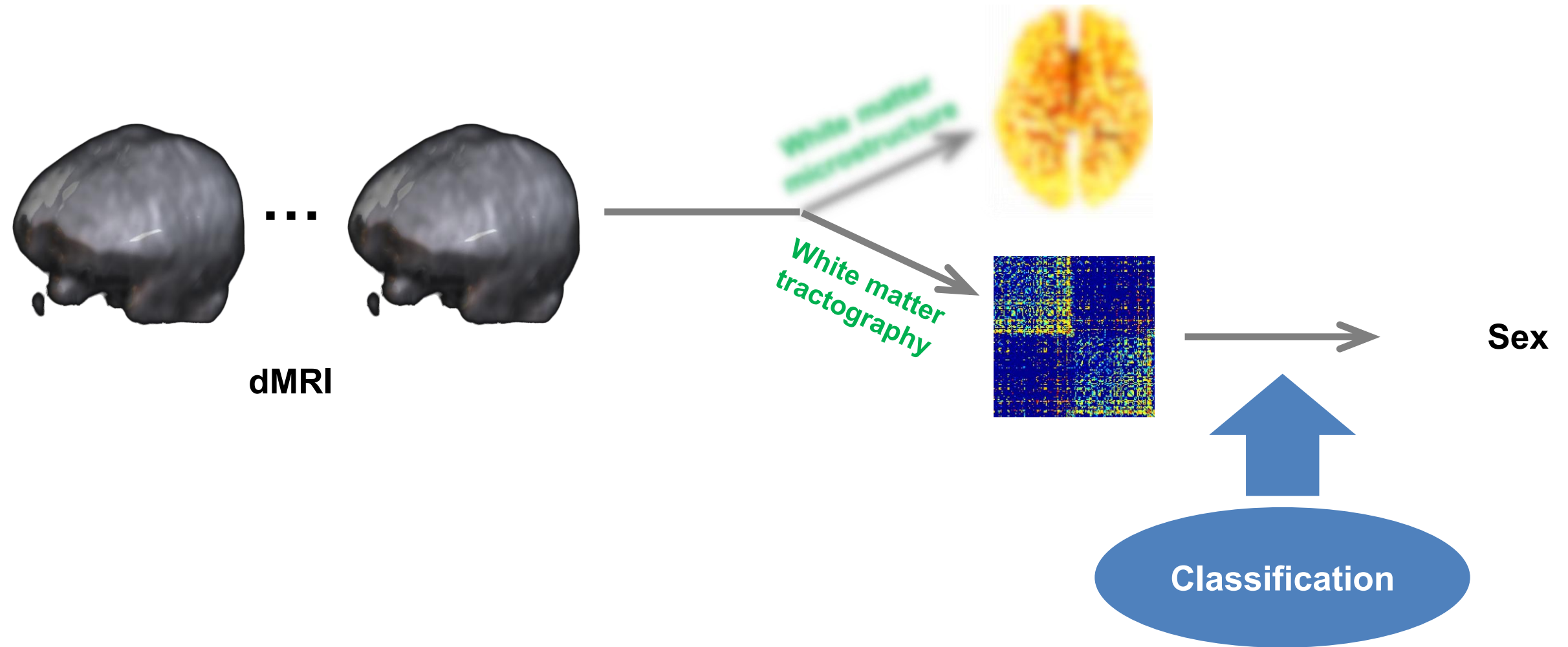


**Functional Brain Network**

- Functional brain networks from resting-state fMRI data
  - Functional connectivity (Pearson correlation (PC)) network
    - Density =  $0.748 \pm 0.108$  ( $0.438 \sim 0.971$ )
  - Effective connectivity (Granger causality (GC)) network
    - Mean time lag =  $2.064 \pm 0.165$  ( $1.481 \sim 2.458$ )
    - Density =  $0.369 \pm 0.130$  ( $0.110 \sim 0.779$ )



**Density of Functional Brain Networks**

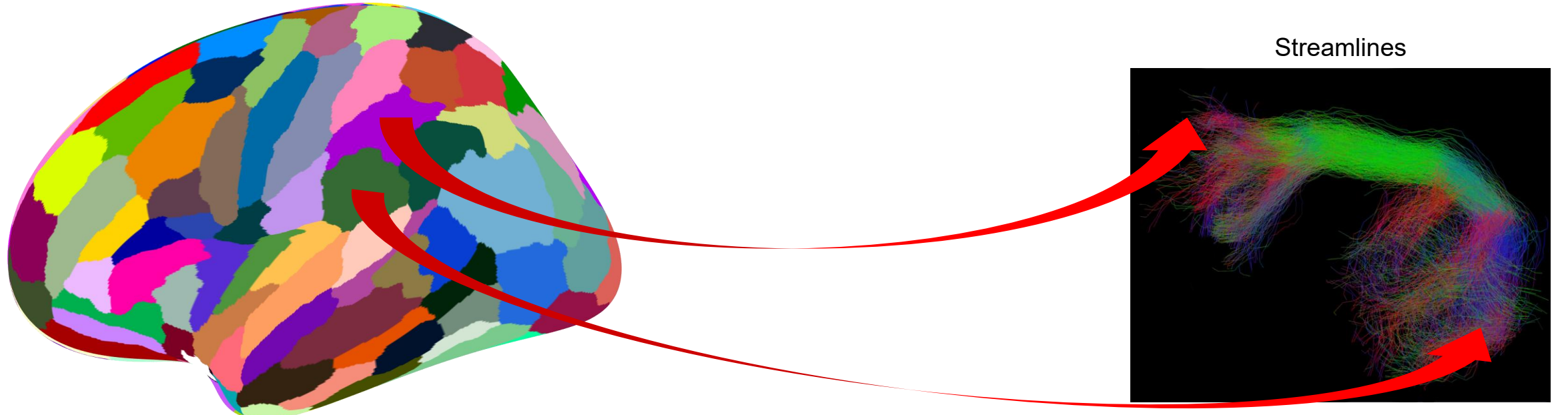


- Preprocessing of dMRI data
  - Correction for head motion, eddy current-induced distortion, and susceptibility artifact (B0 inhomogeneity-induced distortion)
  - Diffusion tensor modelling
  - White matter tractography
  - Construction of structural brain networks



[Fan et al., 2016]

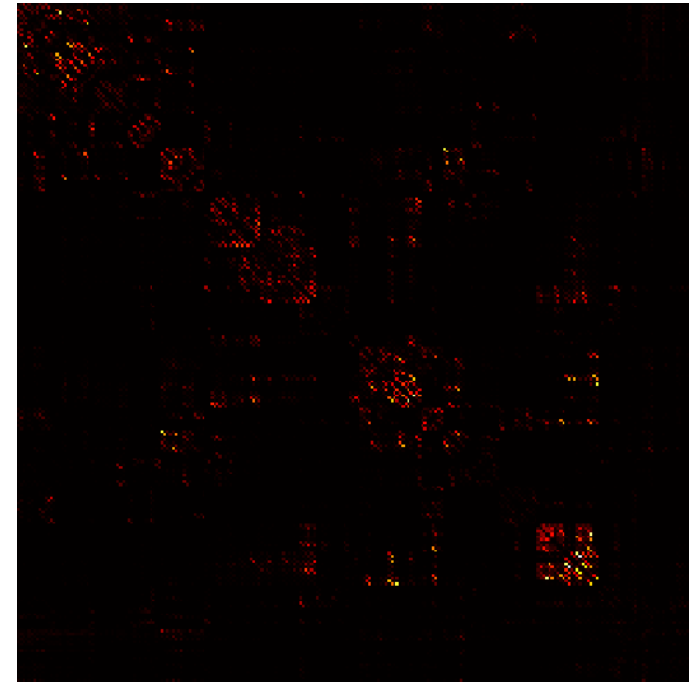
**Definition of 246 Nodes Based on the Brainnetome Atlas**



**Estimation of Edges Between 246 Nodes**

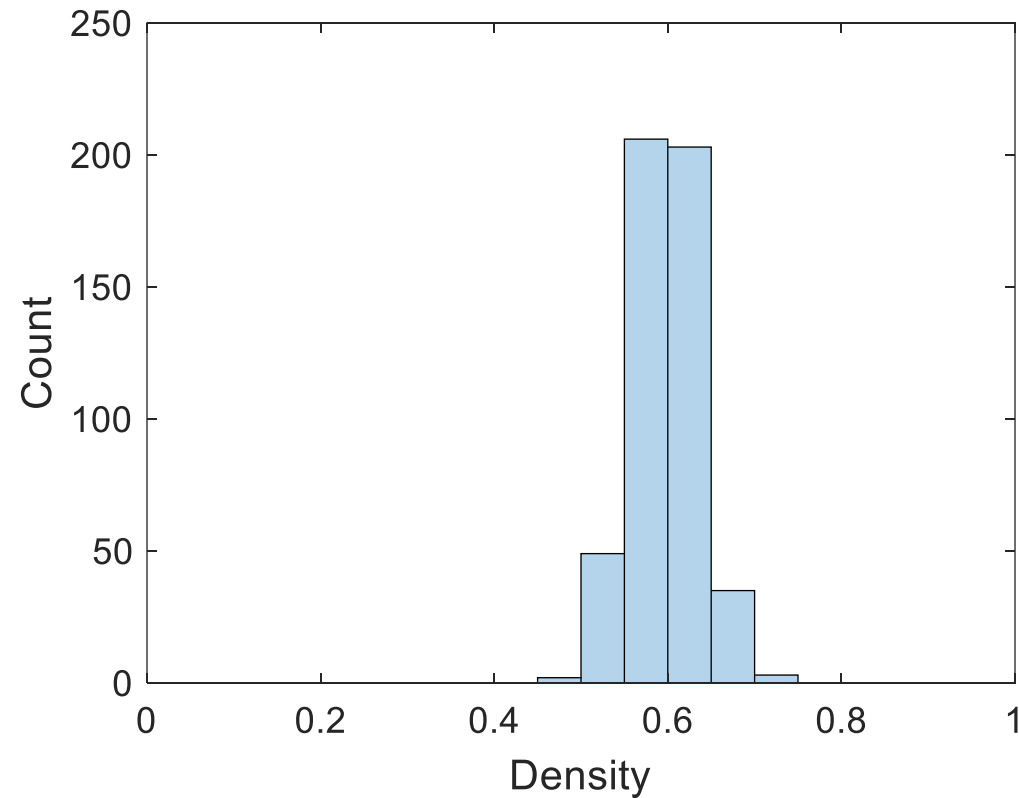


White matter tractography

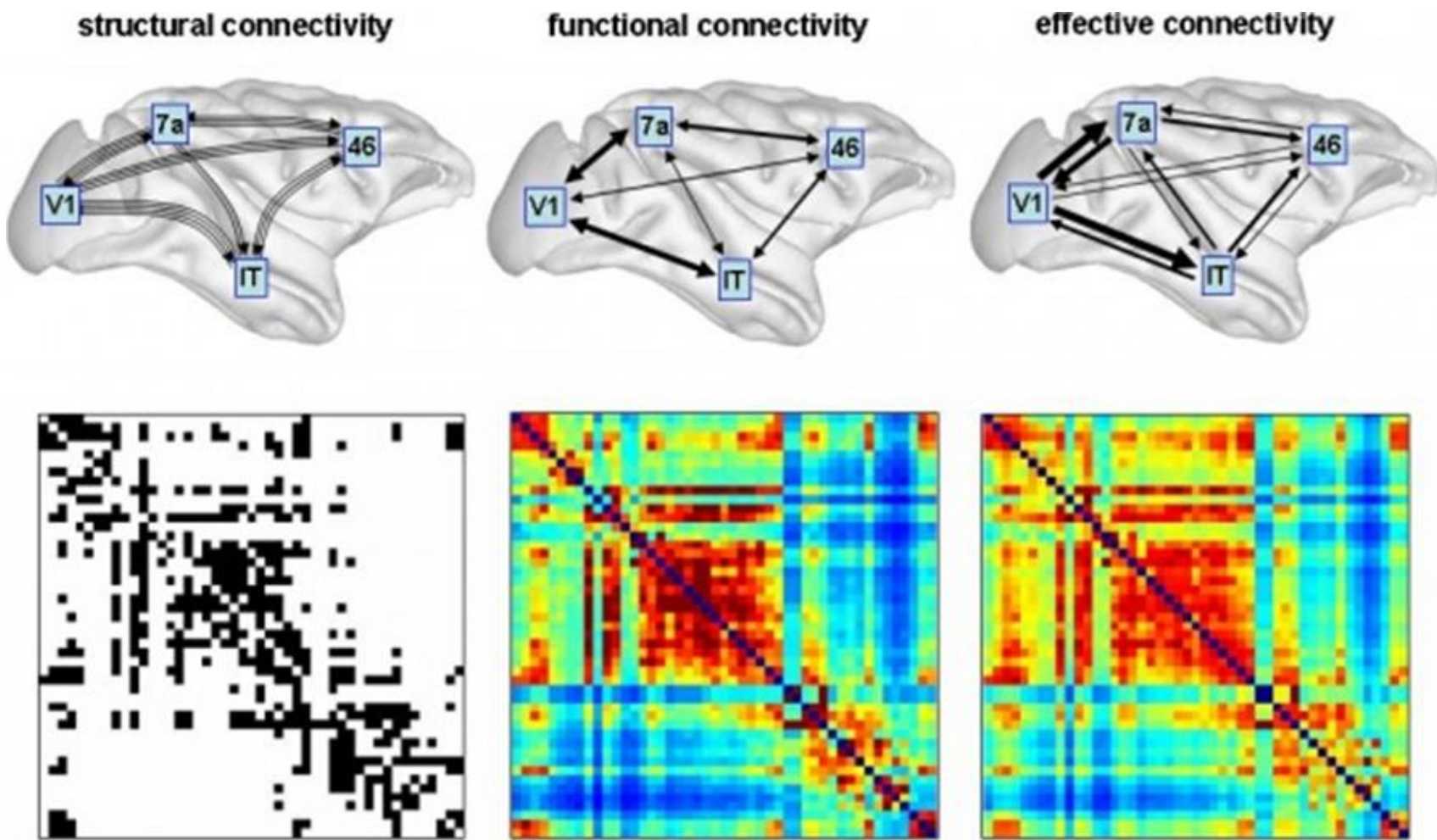


**Structural Brain Network**

- Structural brain networks from dMRI data
  - Structural connectivity (number of streamlines (Count), fractional anisotropy (FA)-weighted, mean diffusivity (MD)-weighted, axial diffusivity (AD)-weighted, or radial diffusivity (RD)-weighted) network
    - Density =  $0.598 \pm 0.038$  ( $0.491 \sim 0.728$ )



## Density of Structural Brain Networks



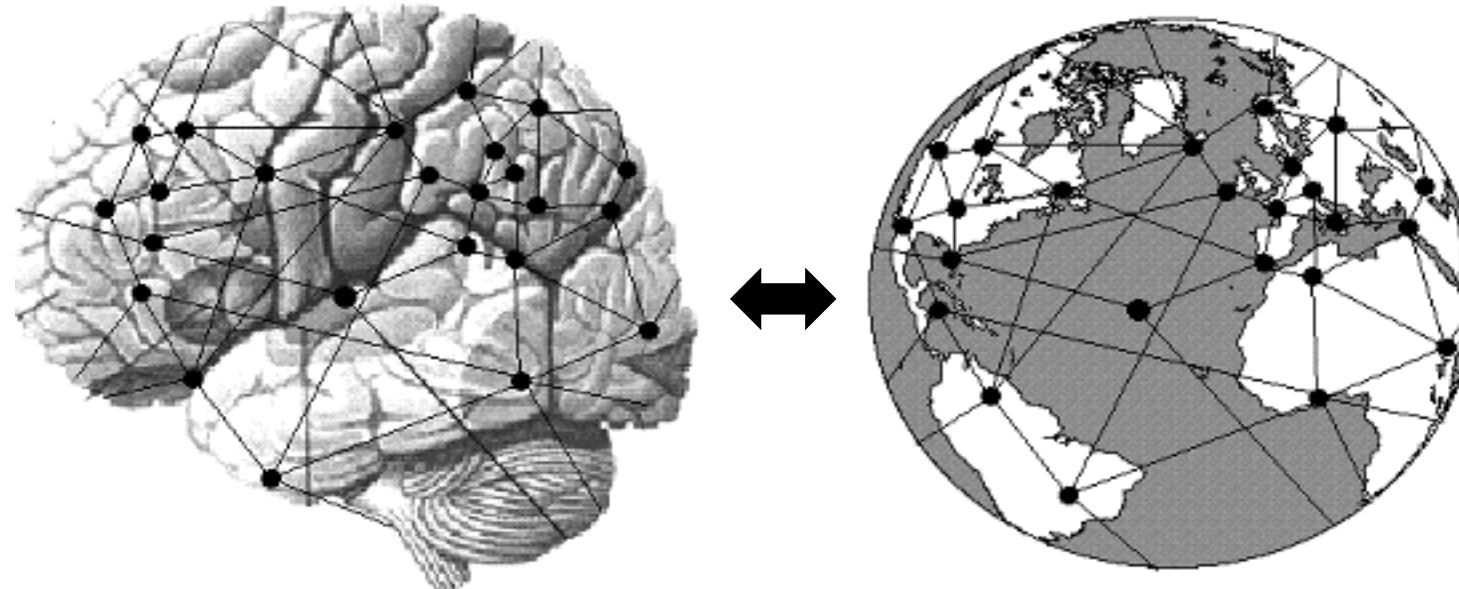
[Honey et al., 2007]

**Three Modes of Brain Connectivity**

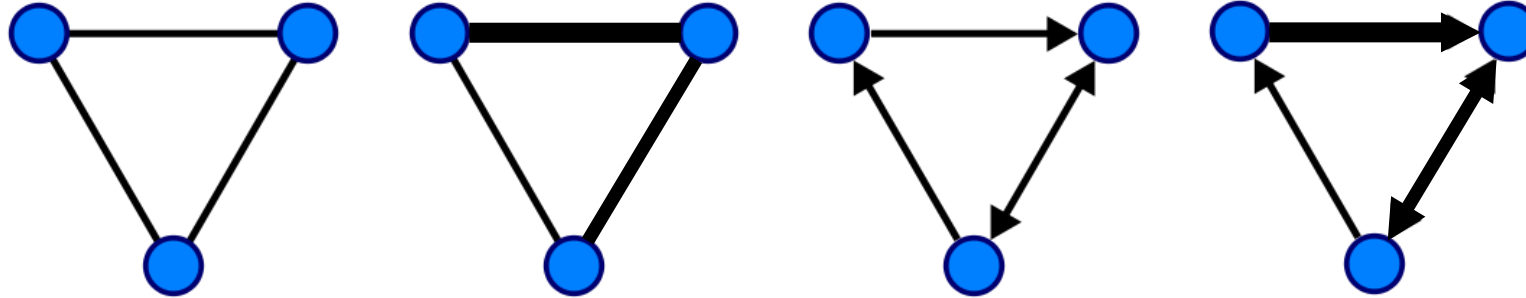
- Target variable
  - Sex (0: female, 1: male)
- Sex classification performance
  - Accuracy for the test set ( $n = 48$ )
    - Proportion of correct classifications
    - Ranges from 0 to 1 (higher is better)

# Graph-theoretical Analysis

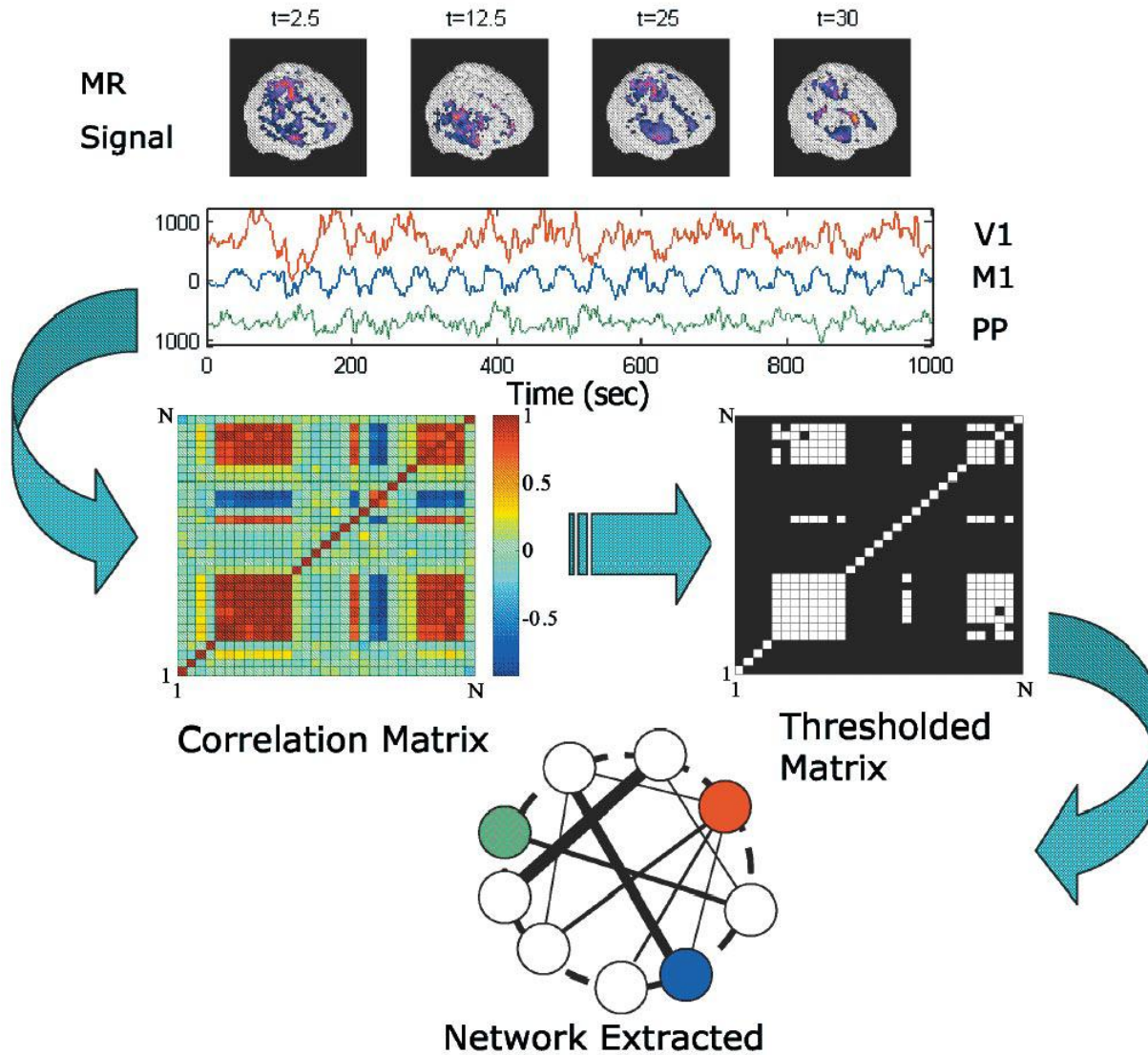
- Allows to conceptualize and analyze the brain as a complex network, similar to other complex networks



- Graph or network
  - Set of nodes and edges
    - Binary or weighted
    - Undirected or directed

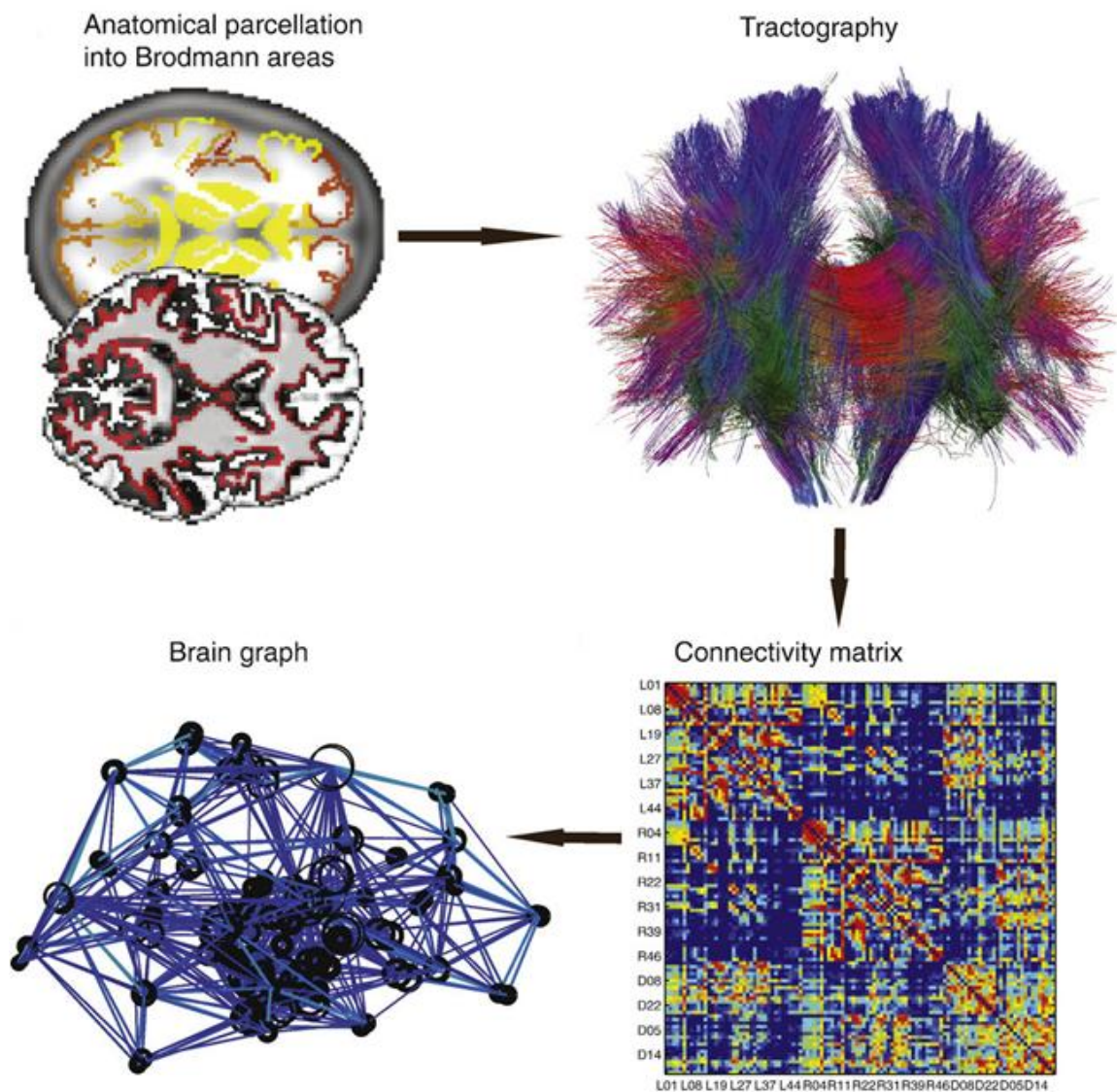


- Construction of brain networks
  - Define nodes
  - Estimate a continuous measure of association between nodes
  - Generate an association matrix by compiling all pairwise associations between nodes
  - If needed, apply a threshold to each element of the matrix to produce a binary matrix



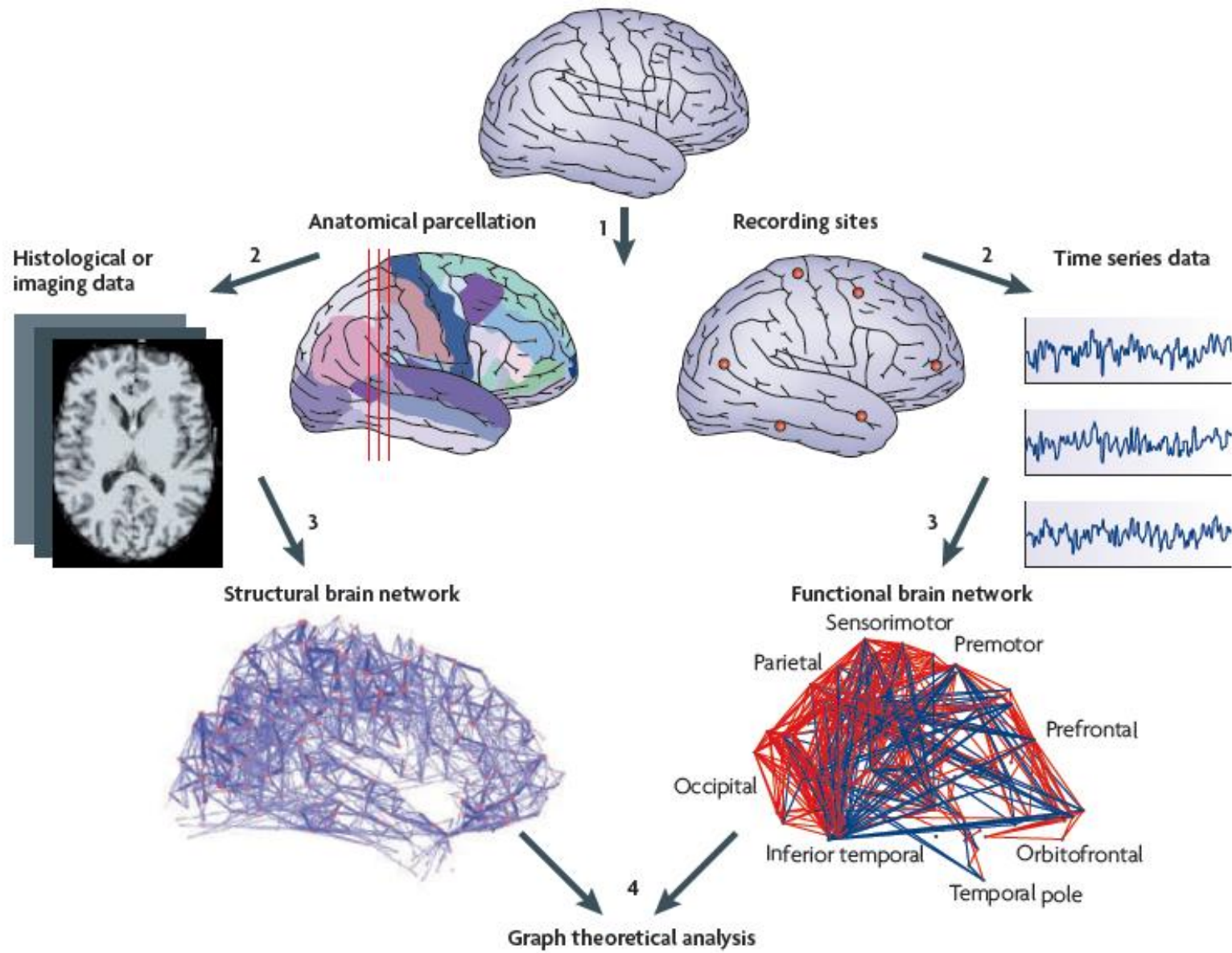
[Eguíluz et al., 2005]

## Construction of Functional Brain Networks



[Vaessen et al., 2010]

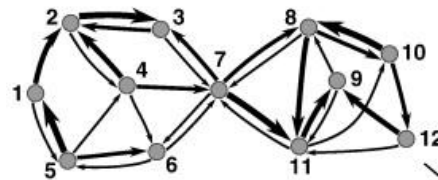
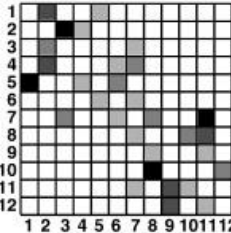
## Construction of Structural Brain Networks



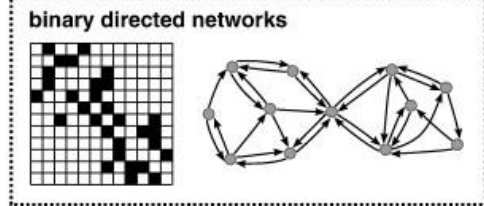
[Bullmore & Sporns, 2009]

## Parallel Construction of Functional and Structural Brain Networks in an Individual

**weighted directed networks**  
structural datasets: tract tracing  
effective datasets: inference of causality  
from functional data

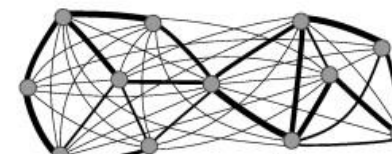
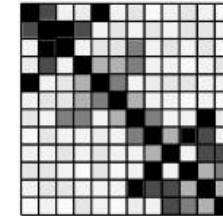


*binarize*

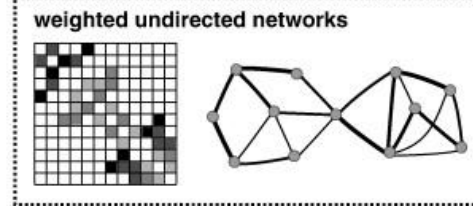


*symmetrize*

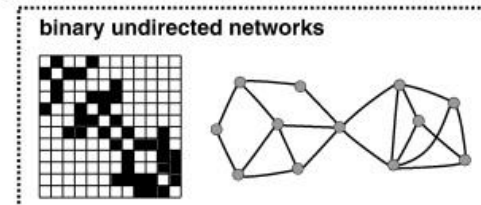
**weighted undirected networks**  
structural datasets: diffusion MRI, structural MRI  
functional datasets: functional MRI, MEG, EEG



*threshold*



*symmetrize*



*binarize*

[Rubinov and Sporns et al., 2010]

## Weighted/Binary Directed/Undirected Networks

- Graph-theoretical analysis
  - Enables to study the brain's organization using the same mathematical principles and metrics used to examine various complex networks across different domains
  - Provides a powerful tool for understanding the brain's connection topology in both health and disease states

### graph theory

clusters / hierarchies, network hubs,  
network summary statistics (e.g. small-worldness, efficiency)

### network modelling from FMRI data

#### functional connectivity

simpler, less meaningful,  
network “discovery”,  
better conditioned,  
can handle more nodes

full correlation

partial correlation

regularised partial correlation

Bayes nets

SEM

non-biological dynamic Bayes nets

#### effective connectivity

more complex, more meaningful,  
pre-specify (constrain) network model,  
harder to estimate,  
can handle fewer nodes

biophysical neural-groups to FMRI-signal forward  
model, fit to data using Bayes (e.g. DCM)

### bottom-up neural network simulations

network of individual  
neurons simulated

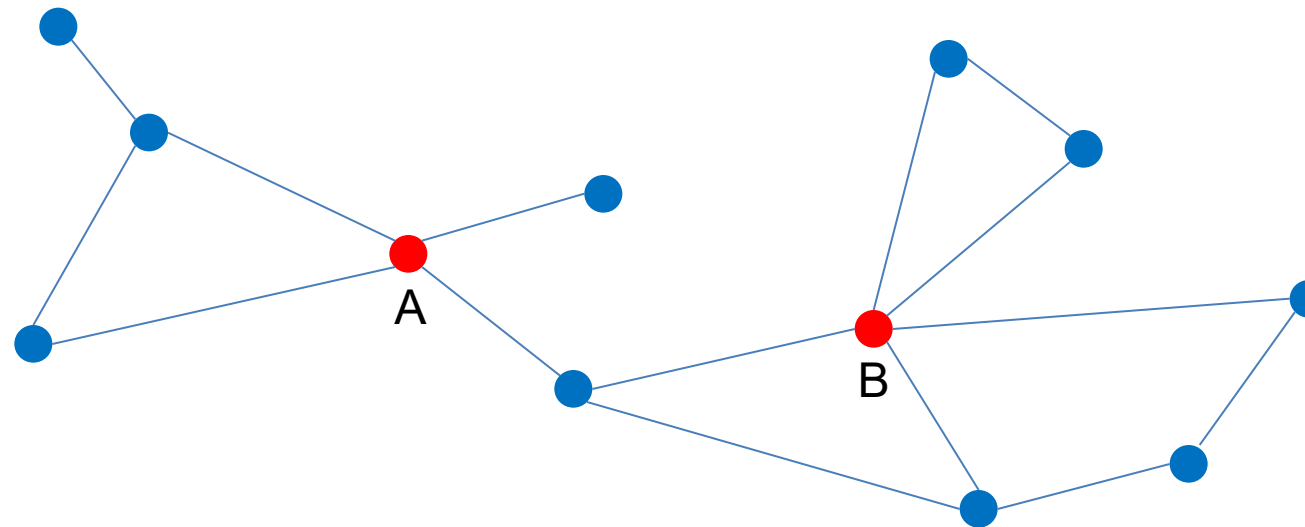
network of groups of  
neurons simulated  
(e.g. neural mass model)

closeness to (interaction with) real FMRI data

[Smith, 2012]

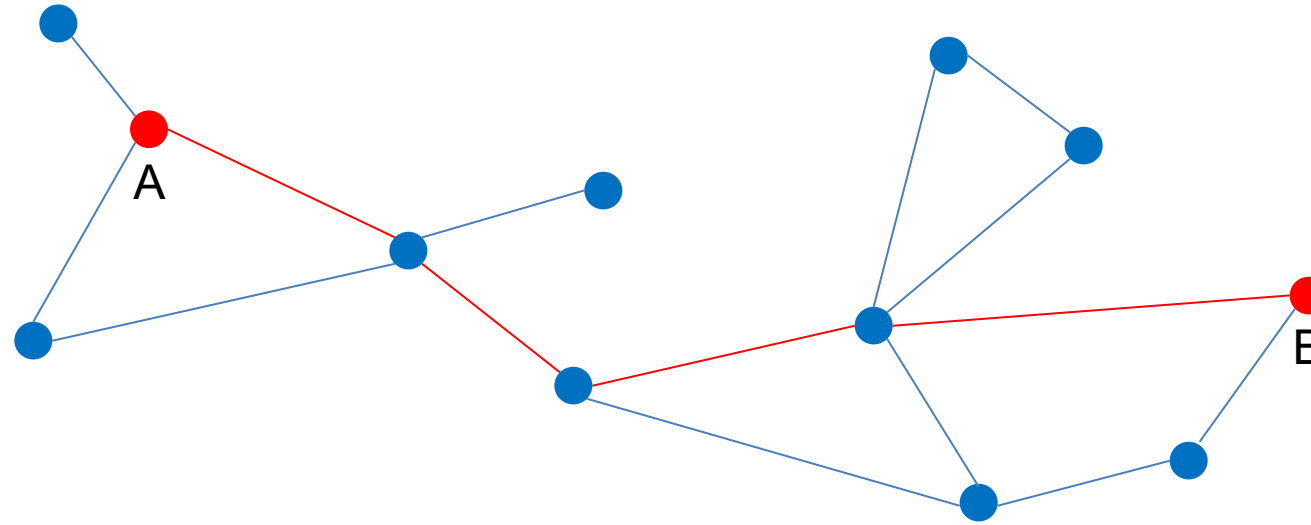
## Bridging Graph-theoretical Analysis and Network Modeling of the Brain

- Network metrics
  - Degree (of a node): number of edges incident to a node



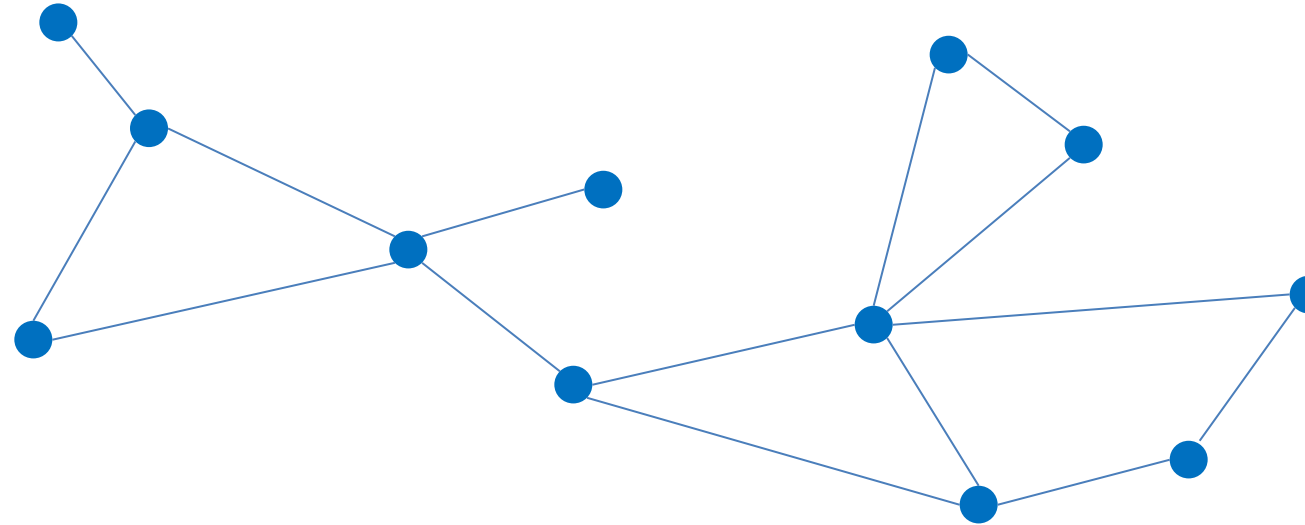
- Degree of node A = 4
- Degree of node B = 5

- Efficiency (in the communication between nodes): inverse of the shortest distance between a pair of nodes [Latora & Marchiori, 2001]



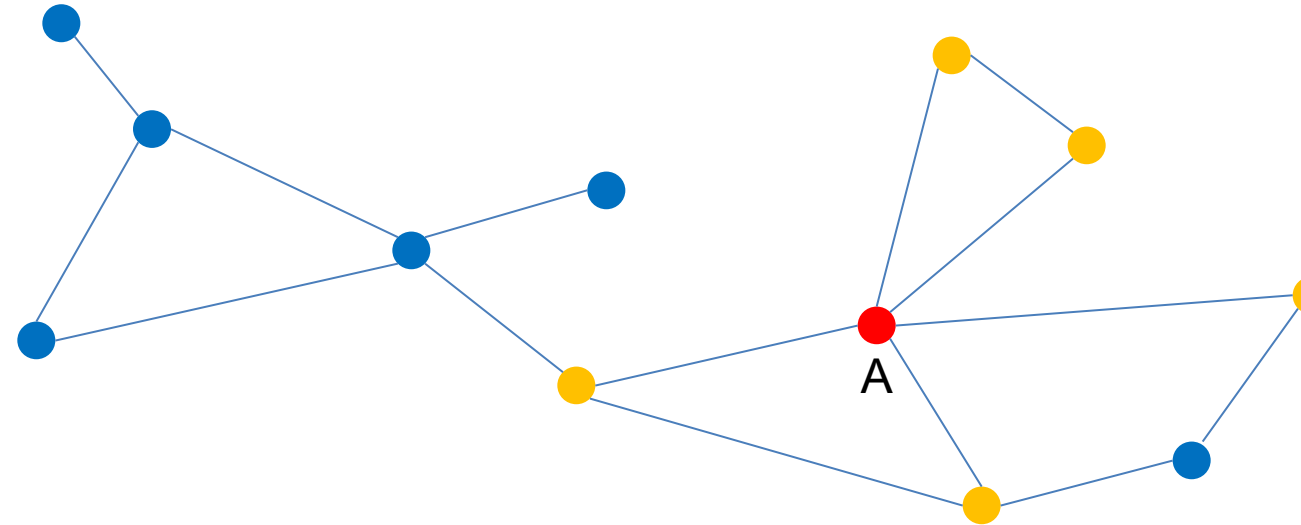
- Shortest distance between nodes A and B = 4
- Efficiency between nodes A and B =  $1/4$

- Global efficiency (of a network),  $E_{\text{glob}}$ : average efficiency across a whole network

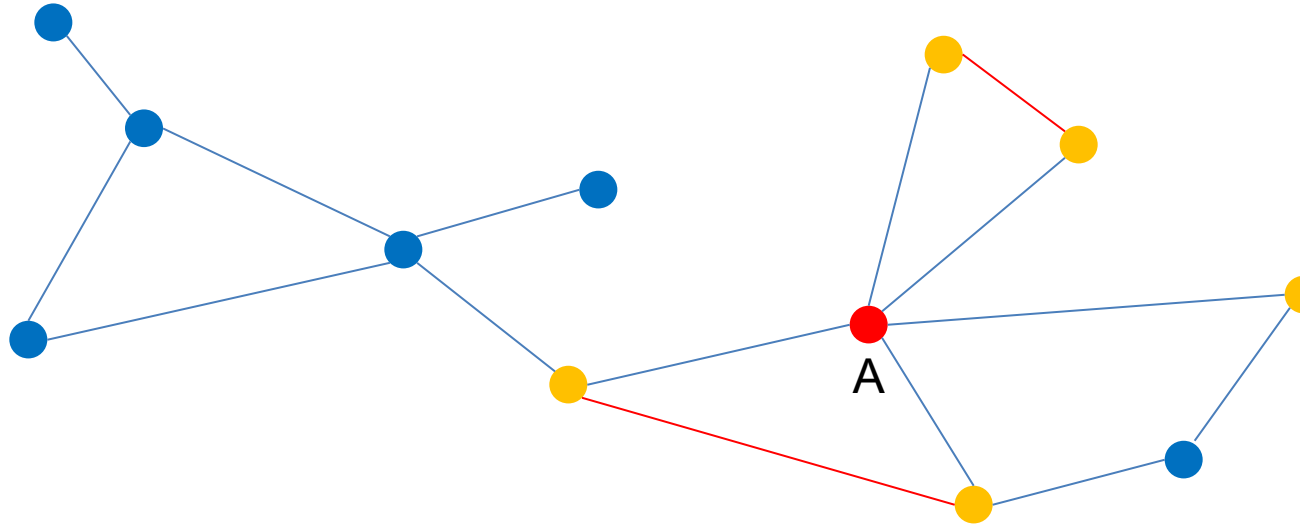


- Represents efficiency in information flow on a global scale

- Nearest neighbors (of a node): nodes adjacent to a node not including itself

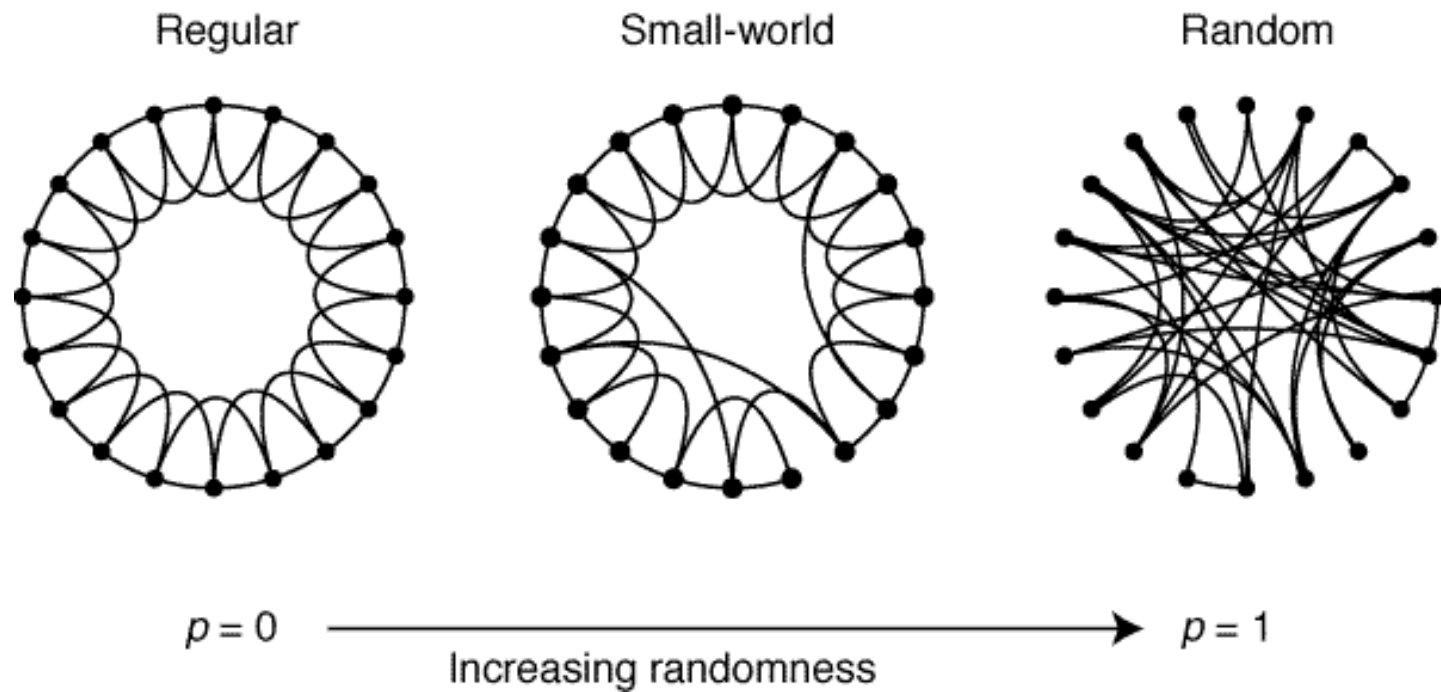


- Efficiency (of a subnetwork): average efficiency across the local subnetwork consisting of the nearest neighbors of a node

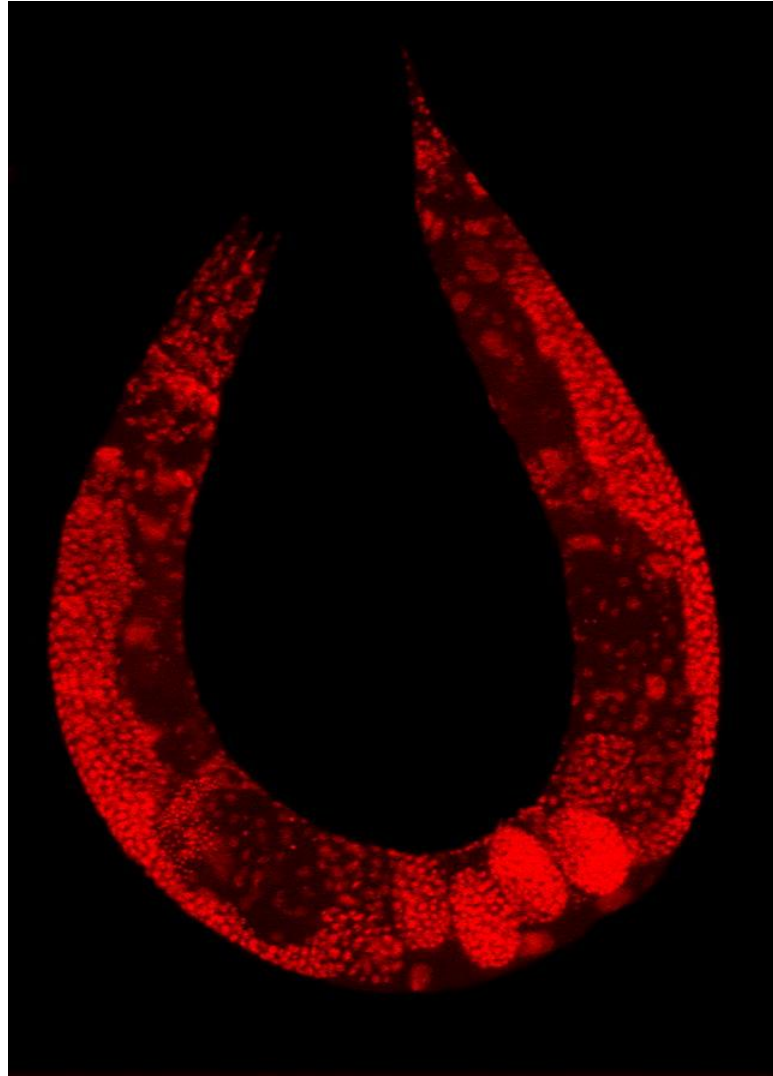


- Local efficiency (of a network),  $E_{\text{loc}}$ : average efficiency of local subnetworks
  - Represents efficiency in information flow on a local scale

- Small-world network
  - Intermediate between regular and random networks
  - Has high global efficiency and local efficiency



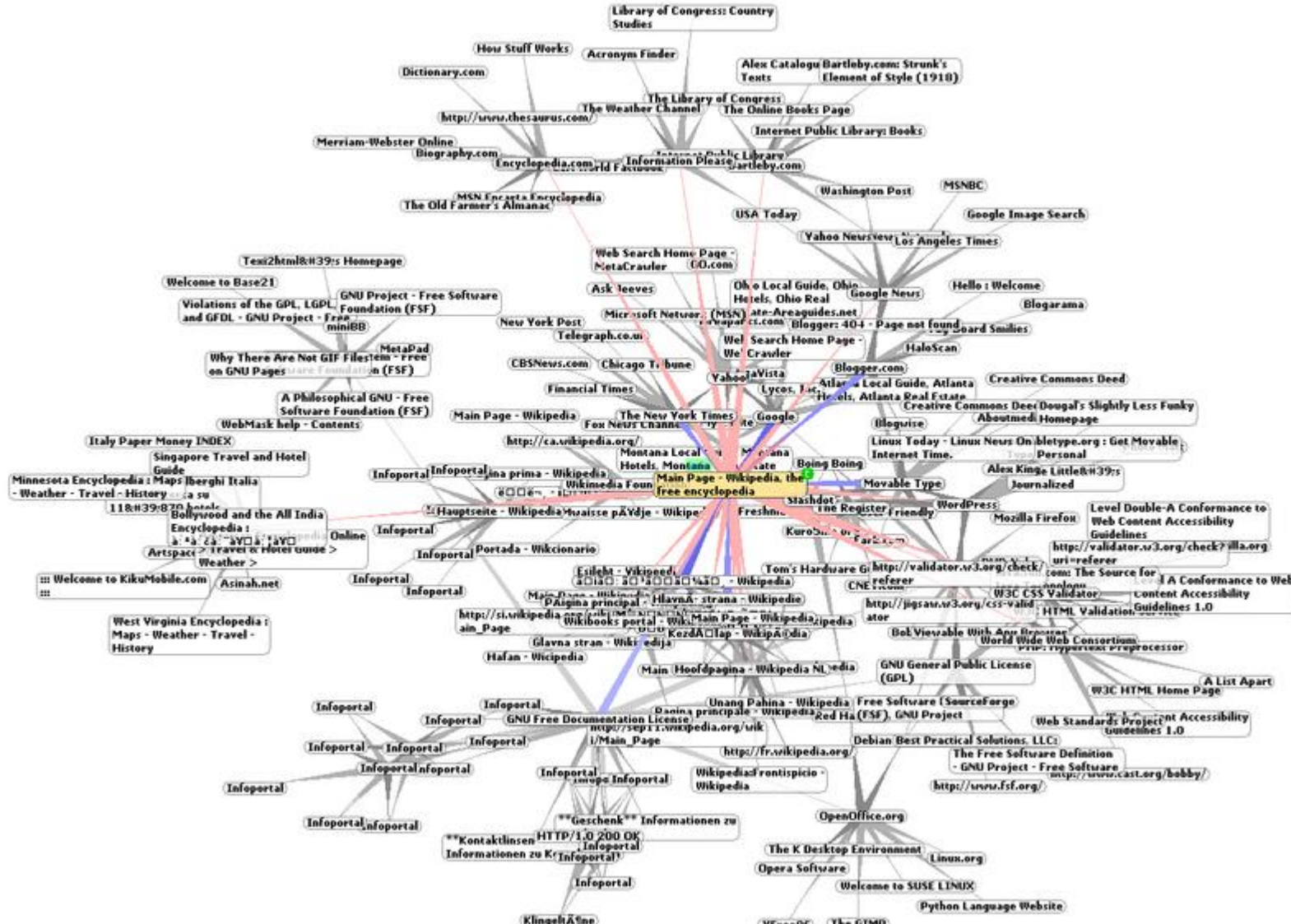
[Watts & Strogatz, 1998]



$$E_{\text{glob}} = 0.46$$
$$E_{\text{loc}} = 0.47$$

[Latora & Marchiori, 2001]

## Small-worldness of Neural Networks: Nervous System of *C. Elegans*



$$\begin{aligned}E_{\text{glob}} &= 0.28 \\E_{\text{loc}} &= 0.36\end{aligned}$$

[Latora & Marchiori, 2001]

# **Small-worldness of Communication Networks: World Wide Web**



**Boston underground transportation system (weighted):**

$$E_{\text{glob}} = 0.63$$

$$E_{\text{loc}} = 0.03$$

**Boston underground transportation system +  
 Boston bus transportation system (weighted):**

$$E_{\text{glob}} = 0.72$$

$$E_{\text{loc}} = 0.46$$

[Latora & Marchiori, 2001]

**Small-worldness of Transport Networks: Boston Transportation System**

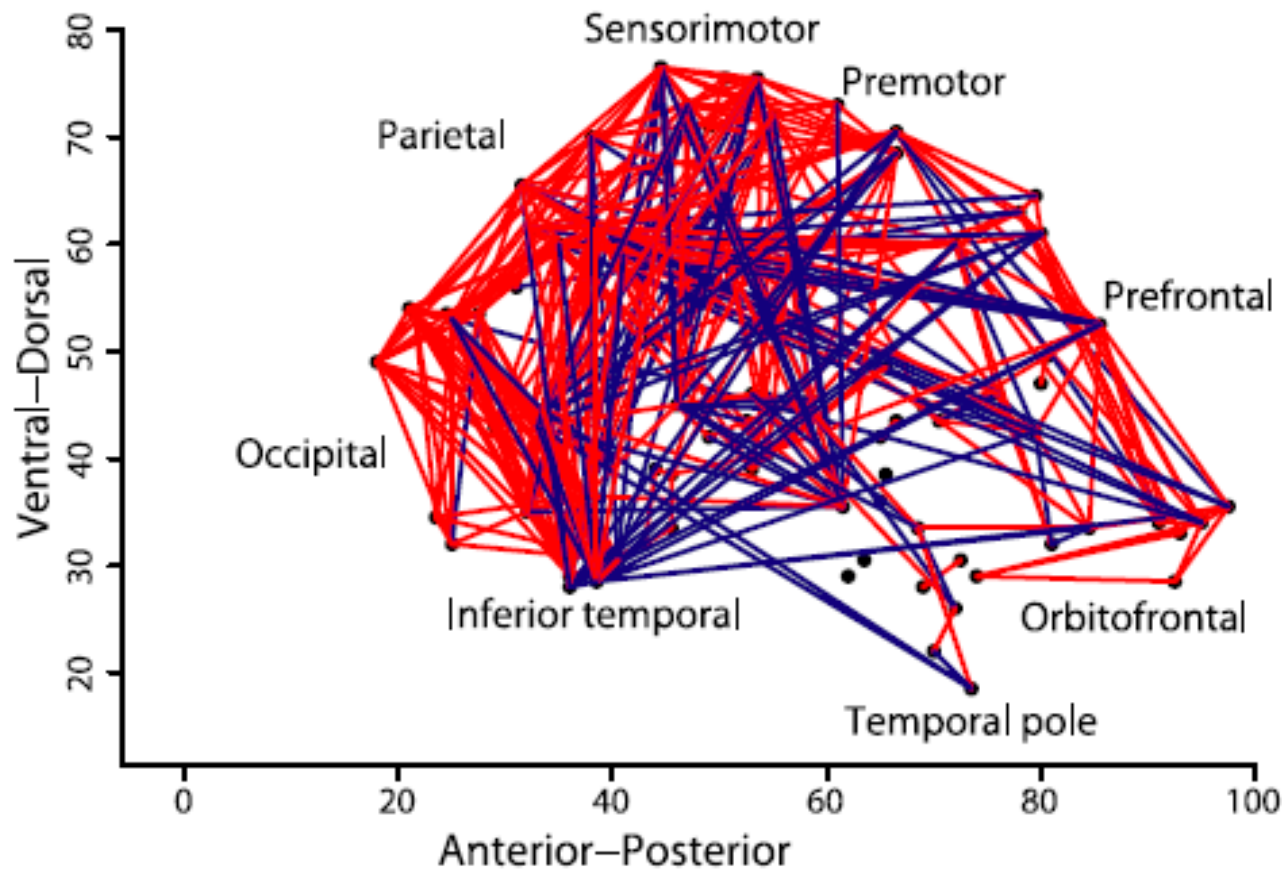
## – Brain as a small-world network

Data	L	C	$\lambda$	$\gamma$	$E_{\text{glob}}$	$E_{\text{loc}}$	Cost
Macaque visual cortex	1.73	0.53	1.04	1.47	—	—	—
Macaque whole cortex	2.38	0.46	1.17	3.06	0.52	0.70	0.18
Cat cortex	1.81	0.55	1.06	1.77	0.69	0.83	0.38

Data	Connectivity Metric	N	k	d	C	L	$\lambda$	$\gamma$	$\sigma$
Macaque cortex (Stephan and others 2000)	Tract-tracing (binary)	39	6.1	0.15	0.38	2.17	1.01	2.46	2.44
Human MEG (Stam 2004)	Synchronization likelihood	126	15	0.12	-0.5	-5.0	-1.8	-4.2	-2.3
Human EEG (Micheloyannis and others 2006)	Synchronization likelihood	28	5	0.18	-0.4	-4.1	-1.0	-2.0	-2.0
Human fMRI (Eguíluz and others 2005)	Correlation	31,503	13.4	$4.3 \cdot 10^{-4}$	0.14	11.4	2.92	325	111
Human fMRI (Salvador, Suckling, Coleman, and others 2005)	Partial correlation	90	5.7	0.06	0.25	2.82	1.09	2.08	1.91
Human fMRI (Achard and others 2006)	Wavelet correlation	90	4.5	0.05	0.53	2.49	1.09	2.37	2.18

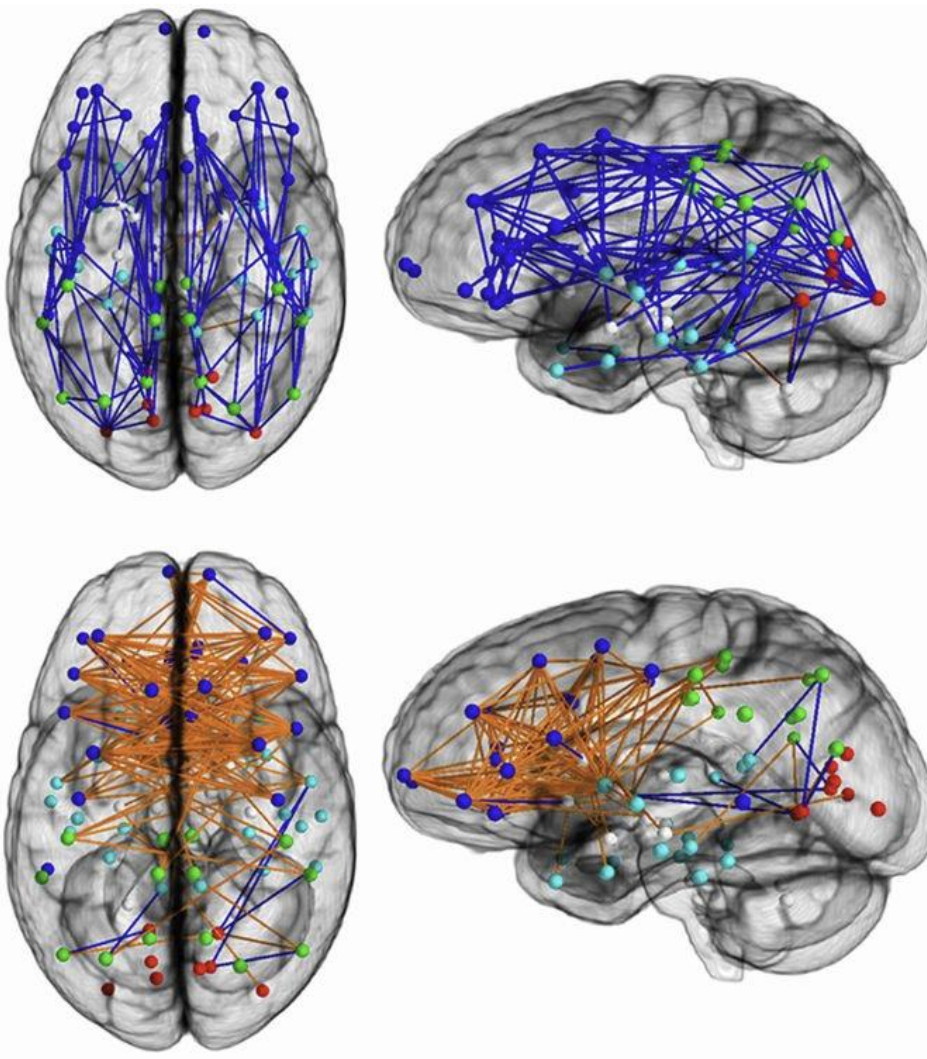
[Bassett & Bullmore, 2006]



[Achard et al., 2006]

## Small-worldness of the Human Brain

- Sex differences in graph-theoretic properties of brain networks
  - Males tend to show higher global efficiency, suggesting more efficient long-range connectivity or more randomization  
[\[Ingalhalikar et al., 2014; Yang et al., 2022\]](#)
  - Females tend to display higher local efficiency, reflecting enhanced local clustering or more regularization  
[\[Sun et al., 2015\]](#)
  - Both sexes exhibit small-world network organization  
[\[Sun et al., 2015\]](#)
  - Results vary considerably across studies depending on imaging modality, network construction methods, sample demographics, and analytical approaches



[Ingalhalikar et al., 2014]

## Sex Differences in Structural Brain Networks: Males vs. Females

Sample	Neuroimaging methods	Main findings on sex differences in brain networks
10 males and 10 females (aged 21-25 years)	rs-fMRI	No significant difference in Eglob and Eloc between males and females (greater Eglob in males and greater Eloc in females)
49 older adults (age mean= 67.25y, 29 women).	rs-fMRI	More regularization in females (Increased Eloc and lower Eglob in females; higher Eglob in males)
10 males and 17 females (aged 5-18 years)	high-density rs-EEG	Alpha frequency band: no differences (low samples) but seems more regularization in males (higher Lp, Cp, $\sigma$ ); beta frequency band: more regularization in females (higher Cp, Lp, $\sigma$ , Eglob)
24 boys and 36 girls (5.7–18.4 years)	rs-fMRI	More regularization in females (higher Lp, $\lambda$ , Cp and Eloc but lower Eglob)
24 females (mean age 39) and 21 males (mean age 45)	EEG	More regularization in females' right-hemispheric (greater right-hemispheric Eloc and lower Eglob)
220 healthy volunteers (aged 7-84 years)	rs-MEG	Similar efficiencies between both males and females
35 females and 35 males (mean age $\pm$ SD = 22.4 $\pm$ 2.3 years)	EEG	More regularization in females (higher Eloc in the delta band when focusing on the search task)

[Zhou & Long, 2024]

## Topological Sex Differences in Functional Brain Networks

Sample	Neuroimaging methods	Main findings on sex differences in brain networks
47 males and 48 females (aged 19–85 years)	DTI	Stronger small-worldization in females (higher Eglob and Eloc)
A healthy sample of 28,821 from UKBB (15,073 females, 13,748 males)	(based on cortical thickness) T1WI	More randomization in males (higher Eglob)
Baseline: 28 females (aged 18-25 years) and 43 males (aged 22-53y) Longitudinal: 15 females (aged 26-61 years) and 13 males (aged 29-53y)	DTI	Stronger small-worldization in males (greater Eglob, lower Lp and increased Cp); weaker small-worldization in females (higher Lp and decreased Cp)
264 males and 391 females (aged 18-35 years)	DWI	More randomization in females (lower Cp)
150 females and 135 males (aged 22-36 years)	(based on cortical thickness) T1WI	More regularization in males (greater Eloc and lower Eglob in the left hemispheric network); more randomized in females (greater Eglob and lower Eloc in the left hemispheric network)
111 females and 61 males (aged 20-65 years)	(based on cortical volume) T1WI	More randomization in females (higher Eglob of structural covariance networks)
99 children (54% boys, aged 6-11 years)	DTI	No significant differences in the structural connectivity and global network properties between male and female children
38 females (aged 18-24 years) and 35 males (aged 18-27y)	DTI	More regularization in females (greater Eloc)
310 twins and their older siblings (158 boys and 172 girls but 20 of them with poor quality DTI scan); mean ages: 10, 13, and 18 years	DTI	No significant sex differences

[Zhou & Long, 2024]

## Topological Sex Differences in Structural Brain Networks

- Network metrics for functional brain networks
  - Edge-wise efficiencies of a binary undirected network (FuncBU\_GE)
  - Node-wise subnetwork efficiencies of a binary undirected network (FuncBU\_LE)
  - Edge-wise efficiencies of a binary directed network (FuncBD\_GE)
  - Node-wise subnetwork efficiencies of a binary directed network (FuncBD\_LE)
- Network metrics for structural brain networks
  - Edge-wise efficiencies of a binary undirected network (StruBU\_GE)
  - Node-wise subnetwork efficiencies of a binary undirected network (StruBU\_LE)